Journal of Visualized Experiments

Generation and Quantitative Characterization of Functional and Polarized Biliary Epithelial Cysts

--Manuscript Draft--

Article Type:	Invited Methods Article - JoVE Produced Video
Manuscript Number:	JoVE61404R2
Full Title:	Generation and Quantitative Characterization of Functional and Polarized Biliary Epithelial Cysts
Section/Category:	JoVE Biology
Keywords:	cholangiocytes, self-organization, lumen, cell polarity, cysts, organogenesis, bile ducts
Corresponding Author:	Pascale Dupuis-Williams INSERM Orsay, FRANCE
Corresponding Author's Institution:	INSERM
Corresponding Author E-Mail:	pascale.dupuis-williams@universite-paris-saclay.fr
Order of Authors:	Latifa Bouzhir
	Emilie Gontran
	Lorena Loarca
	Mauricette Collado-Hilly
	Pascale Dupuis-Williams
Additional Information:	
Question	**Response**
Please indicate whether this article will be Standard Access or Open Access.	Standard Access (US$2,400)
Please indicate the **city, state/province, and country** where this article will be **filmed**. Please do not use abbreviations.	Orsay, France

TITLE:

Generation and Quantitative Characterization of Functional and Polarized Biliary Epithelial Cysts

AUTHORS AND AFFILIATIONS:

Latifa Bouzhir*[1], Emilie Gontran*[1], Lorena Loarca[1], Mauricette Collado-Hilly[1], Pascale Dupuis-Williams[1,2]

[1]Université Paris-Saclay, Inserm U1193, Physiopathogénèse et traitement des maladies du foie, Orsay, Cedex, France
[2]ESPCI Paris – PSL 10, rue Vauquelin, Paris Cedex 05 France

*These authors contributed equally

Corresponding Author:
Pascale Dupuis-Williams (pascale.dupuis-williams@universite-paris-saclay.fr)

E-mail Addresses of Co-authors:
Latifa Bouzhir (latifa.bouzhir@universite-paris-saclay.fr)
Emilie Gontran (emilie.gontran@universite-paris-saclay.fr)
Lorena Loarca (lorena.loarca@universite-paris-saclay.fr)
Mauricette Collado-Hilly (mauricette.collado-hilly@universite-paris-saclay.fr)

KEYWORDS:
cholangiocytes, self-organization, lumen, cell polarity, cysts, organogenesis, bile ducts

SUMMARY:
Three-dimensional (3D) cellular systems are relevant models for investigating organogenesis. A hydrogel-based method for biliary cysts production and their characterization is proposed. This protocol unravels the barriers of 3D characterization, with a straightforward and reliable method to assess cyst formation efficiency, sizes, and to test their functionality.

ABSTRACT:
Cholangiocytes, the epithelial cells that line up the bile ducts in the liver, oversee bile formation and modification. In the last twenty years, in the context of liver diseases, 3D models based on cholangiocytes have emerged such as cysts, spheroids, or tube-like structures to mimic tissue topology for organogenesis, disease modeling, and drug screening studies. These structures have been mainly obtained by embedding cholangiocytes in a hydrogel. The main purpose was to study self-organization by addressing epithelial polarity, functional, and morphological properties. However, very few studies focus on cyst formation efficiency. When this is the case, the efficiency is often quantified from images of a single plane. Functional assays and structural analysis are performed without representing the potential heterogeneity of cyst distribution arising from hydrogel polymerization heterogeneities and side effects. Therefore, the quantitative analysis, when done, cannot be used for comparison from one article to another.

Moreover, this methodology does not allow comparisons of 3D growth potential of different matrices and cell types. Additionally, there is no mention of the experimental troubleshooting for immunostaining cysts. In this article, we provide a reliable and universal method to show that the initial cell distribution is related to the heterogeneous vertical distribution of cyst formation. Cholangiocyte cells embedded in hydrogel are followed with Z-stacks analysis along the hydrogel depth over the time course of 10 days. With this method, a robust kinetics of cyst formation efficiency and growth is obtained. We also present methods to evaluate cyst polarity and secretory function. Finally, additional tips for optimizing immunostaining protocols are provided in order to limit cyst collapse for imaging. This approach can be applied to other 3D cell culture studies, thus opening the possibilities to compare one system to another.

INTRODUCTION:

In the last three decades, the field of in vitro research has advanced towards 3D culture systems. A number of protocols have emerged for culturing cells in 3D as spheroids or aggregates in the presence or absence of a scaffold/matrix, in a drop, in agitation, in microfluidic devices, or floating[1]. The use of 3D culture methods has proved its advantages over 2-dimensional (2D) cultures, particularly for epithelial cells, which were shown to self-organize in 3D structures, called cysts or acini. In this case, the cells form a monolayer encircling a lumen, where cells acquire their full epithelial phenotype with improved physiological specific functions[2].

Numerous studies have contributed to the development of methods for forming these epithelial organoids in natural matrices. This has allowed to recapitulate in vivo cell-cell and cell-microenvironment interactions, to get the establishment and the stability of the epithelial phenotype[3-7]. Recently, and in particular with the aim of developing transplantable organoids and deciphering the requirement of the microenvironment for orchestrating the epithelial program, synthetic hydrogels have been developed to enhance the formation of epithelial acini[8-10]. Unfortunately, these studies report on qualitative data, or present calculation methods using internal references such as the ratio of cysts over non-cysts in a 2D plane[8-10]. This precludes any comparison between different studies in terms of efficiency, stability, or morphological and physiological characterization of the epithelial organoids.

Microencapsulation of epithelial cells in beads using microfluidic devices has allowed for more realistic quantitative and comparative results. Using this technology, organoids from various cell types were formed and differentiated based on the morphology among different 3D cellular structures[11,12]. However, this technology is not easy to work with and requires the use of clean rooms to produce the microfluidic devices. This technology has been established for a few types of hydrogels but requires technical adaptation to be applied to other hydrogels, restricting its versatility. Therefore, most studies intended to develop epithelial organoids rely on the embedding of epithelial cells in a hydrogel bulk. In these methods, the high heterogeneity of gel structuration and cell distribution inside the whole 3D culture is often neglected. Therefore, most of the analyses relate to single 2D images, which represent only very roughly the distribution of the various cellular objects in the whole 3D volume.

Diseases that affect bile ducts, such as cholangiocarcinoma, biliary atresia, primary sclerosing

cholangitis, among others, are a major cause of mortality and morbidity. Except for liver transplantation, there are no effective treatments for these conditions[13]. Efforts to investigate bile duct formation, disease causes, and progression will allow the development of novel therapies[14].

Biliary organotypic models of cysts, spheroids or tube-like structures using normal or patient-derived, differentiated, or progenitor-derived cholangiocyte cell lines have been developed[15-20]. Various studies have recapitulated cholangiocyte polarity, expression of cholangiocyte markers, presence of cilia, cholangiocyte secretory and reabsorptive ability, and lumen formation and obstruction; all of which represent important characteristics of cholangiocyte phenotype, morphology, and function[15,17,19]. Others have reported maintenance of patient-derived biliary organoids for long periods of time[20]. Recently, we investigated the role of biochemical and biophysical cues on biliary cysts organogenesis[21]. Importantly, the pathogenesis of biliary atresia was studied in biliary spheroids and tubes[7,22]. Furthermore, key features of primary sclerosing cholangitis such as cholangiocyte senescence, secretion of pro-inflammatory cytokines, as well as macrophage recruitment were successfully studied using biliary spheroids[15,20]. However, reproducible in vitro 3D quantitative models that physiologically modulate cholangiocyte phenotype, physiology, and microenvironment where these questions can be addressed are still needed. Moreover, only few publications have reported cyst formation efficiency[21,23]. This is an important point to establish, particularly when investigating organogenesis, disease cause, and correlation of drug responses with cholangiocyte function and polarization. In addition, with differences in scaffold/matrix used from protocol to protocol, it is difficult to compare between systems. To solve these issues, we propose a quantitative, reliable, and universal method to generate biliary cysts mimicking lumen formation, cholangiocyte polarization, and cholangiocyte secretory function. Importantly, we present a systematic analysis performed along the Z-axis across the 3D gel when evaluating over time, cyst formation efficiency, size, viability, polarization, and functionality. Furthermore, we used a natural hydrogel and normal rat cholangiocytes (NRC)s, as an example for the protocol, but other natural or synthetic hydrogels, as well as epithelial cells could be used for the formation of 3D cystic structures.

PROTOCOL:

1. Generation of cysts

NOTE: This protocol can be performed with any type of hydrogel, if the gelation allows embedding of cells.

1.1. Hydrogel coating

NOTE: Proper hydrogel coating of the chamber slide is a critical step to avoid the formation of 2D cell layers on the bottom of the well, that might interfere with subsequent cyst imaging and impair the calculation of cyst formation efficiency.

1.1.1. To ensure homogeneity of the gel solution, thaw the hydrogel at 4 °C overnight (O/N).

1.1.2. Precool pipette tips on ice or O/N at -20 °C and 8-well chamber slide at -20 °C O/N.

1.1.3. Place the hydrogel and 8-well chamber slide on an ice bucket filled with ice.

1.1.4. In a 15 mL conical tube, prepare a solution containing 40% hydrogel (V/V) in cold NRC complete medium (see **Table of Materials**) and place the tube on ice.

1.1.5. To coat a chamber slide, using cold pipette tips, add 50 µL of hydrogel solution on the center of each well, and spread over the whole surface using a pipette tip, while holding the chamber slide on ice (**Figure 1A**).

NOTE: Spread the hydrogel solution as evenly as possible avoiding bubbles.

1.1.6. To polymerize the hydrogel, incubate the chamber slide for at least 15 min at 37 °C, 5% CO_2.

1.2. Cell preparation

1.2.1. Warm up NRC complete medium, phosphate buffered saline (PBS), and trypsin-ethylenediamine tetraacetic acid (trypsin-EDTA) in a water bath pre-heated to 37 °C.

1.2.2 While the hydrogel is polymerizing, ensure that NRCs are grown to 70% confluency in a T-25 cm^2 collagen-coated flask[21]. Wash the cells once with pre-heated 1x PBS.

1.2.3. Incubate the NRCs with 5 mL of pre-heated 1x PBS (for a T-25 cm^2 flask) for 20 min at 37 °C, 5% CO_2.

NOTE: This step, which shortens the incubation time with trypsin-EDTA is instrumental in retaining the self-organizing properties of cells.

1.2.4. Discard the PBS, add 1 mL of trypsin-EDTA, and incubate for 5-10 min at 37 °C, 5% CO_2.

1.2.5. Neutralize with 4 mL of pre-heated complete NRC medium. Collect and transfer the cell suspension into a 15 mL conical tube, and spin at 150 *x g* for 4 min.

1.2.6. Discard the medium and resuspend the cell pellet in 5 mL of pre-heated medium.

1.2.7. Using a 40 µm cell strainer, filter the cell solution into a 50 mL conical tube and count the cells.

NOTE: Passing the cells through a strainer is a critical step for the quantitative results to be reproducible i.e., to get almost similar size of cell aggregates to be embedded.

1.3. Embedding of cell suspension in hydrogel solution

1.3.1. Prepare a solution of 1,600 µL of 80% hydrogel (V/V) in cold complete NRC medium (tube 1); keep in ice. Dilute 5 x 10^5 cells/mL in 1,600 µL of cold complete NRC medium (tube 2) and keep on ice.

NOTE: This step must be performed quickly to avoid polymerization of the hydrogel while mixing it with the cell suspension and to maintain cell viability.

1.3.2. To prepare a cell seeding solution of 2.5 x 10^5 cells/mL in 40% hydrogel (V/V), mix tube 1 and tube 2. Add 400 µL of the cell solution into each well of the hydrogel-coated chamber slide avoiding bubbles (**Figure 1B**).

1.3.3. Keep the chamber slide in an incubator at 37 °C with 5% CO_2 until media change.

1.3.4. After 2 days in culture, remove 250 µL of the medium from a corner of each well, be careful to not pipette out the hydrogel. Then, slowly add 250 µL of the culture medium. Change the medium every 2 days.

NOTE: Minimize the movement of the chamber slide, particularly during the cyst initiation.

2. Cyst quantification

2.1. Cyst imaging

NOTE: This section should be performed quickly to not compromise the cell viability if the microscope is not equipped with a heating chamber to control CO_2 and temperature. In order to ensure consistent quantification, representative of the cyst distribution in the full hydrogel volume, cysts are imaged via phase-contrast microscopy and serial imaging (Z-stacks), with pre-defined parameters throughout different time points.

2.1.1. Take a Z-stack along the depth of the hydrogel for each time point (**Figure 1C, D**). In this example, Z-stacks are taken at days 1, 2, 4, 7, and 10.

NOTE: Check that the initial cell distribution is uniform in the hydrogel to ensure the applicability of this method.

2.1.1.1. With a phase-contrast microscope equipped with an image acquisition software, select the 10x objective magnification in the manual nose-piece pad window (**Figure 2B(1)**).

2.1.1.2. Switch on the white lamp and select the brightfield imaging option.

2.1.1.3. Switch the camera on by selecting the "**Play**" button in the bar submenu. Focus on a field of cysts and set the exposure time (**Figure 2B(2)**). Open the **Auto Capture Folder** window for an

automatic saving of images (**Figure 2B(3)**).

2.1.1.4. Open the capture Z-series window and define with the Z screw the top and bottom planes of the Z-stack (same XY coordinates but different Z screened). Adjust the Z-step depending on the objective, the level of resolution and press the button "**Run now**" to launch the acquisition (**Figure 2B(4)**).

NOTE: In this example, cysts are spread over a hydrogel thickness of 520 µm. 26 images are acquired along the hydrogel depth with a 20 µm Z-step interval. Depending on the objective, the Z-step should be adjusted to not miss any cyst and to ensure the detection of single cells and aggregates.

2.1.1.5. Take at least 3 non-overlapping Z-stacks per well.

NOTE: This sampling is necessary when, like in this example, cysts are more numerous in the depth of the gel than on the edges due to heterogeneities in the hydrogel polymerization.

2.1.1.6. In order to have a representative dataset repeat step 2.1.1.5. for 3 wells in total.

NOTE: The heterogeneous distribution of cysts depends on the type of hydrogel, its polymerization, and the cell line. Considering three Z-stacks per well and three wells per experiment, a minimum of 200 cysts are imaged over nine Z-stacks to characterize cyst formation and cyst growth at each time point.

2.2. Image processing

NOTE: In a hydrogel, NRCs can be found as single cells, cysts or aggregates. Cysts are identified by the presence of a round and thin contrasted cell shell enclosing a lumen, while cell aggregates present an irregular shape and do not have a lumen. Aggregates and single cells have a dense and contrasted appearance (**Figure 3B(4)**).

2.2.1. Open the Fiji software, open the Z-stack and go to the Fiji menu and click **File | Open** (**Supplementary Figure 1**). Select the Z-stack to analyze. If needed, select "**Virtual Stack**" option and click "**Yes**" for opening (**Figure 3A(1)**).

2.2.2. Duplicate the stack via **Image | Duplicate.** Click on the box "**Duplicate stack**" and click "**OK**" (**Supplementary Figure 2**).

NOTE: In this example, Z-stacks are in .nd2 file format encoded in 16 bits.

2.2.3. Create a minimum intensity projection from the duplicated stack. Go to the **Image menu | Stacks | Z Project**. Select Projection type "**Min Intensity**" and click "**OK**" (**Figure 3A(2)**) (**Supplementary Figure 3**).

2.2.4. Subtract the background from the projection. Go to the **Process menu | Subtract Background**. Type 500.0 pixels of rolling ball radius and click "**light background**" to render cysts more contrasted than the background (**Figure 3A(3)**) (**Supplementary Figure 4**).

NOTE: The rolling ball radius defines the size of the region on which background subtraction is operated. This parameter must be set to the size of the largest object to identify.

2.2.5. If contrast enhancement is needed, go to **Image menu | Adjust | Brightness/Contrast | Auto | Apply**. Fiji will automatically optimize brightness and contrast. In (**Figure 3A(3)**), the lower and upper gray values were set to 49702 and 65452, respectively (**Supplementary Figure 5**).

NOTE: If the projection is not calibrated, go to the **Analyze menu | Set scale** and type the corresponding calibration µm/pixel ratio (**Supplementary Figure 6**).

2.3. Cyst counting and cyst size measurements

2.3.1. To measure the approximate cyst diameter, select the **Straight-line** tool in the Fiji menu and draw a line across the diameter of each cyst on the final projection (**Figure 3B(4)**). Add the new region of interest (ROI) created for each cyst to the ROI manager: press the "**t**" shortcut on the keyboard for faster counting and opening of the ROI manager. Click "**Show All**" to see the counted cysts (**Supplementary Figure 7**)

2.3.2. Check that no cyst has been left without counting by superimposing the set ROIs from the projection on the Z-stack. To do so, click on the **Z-stack window** to select it. In the ROI Manager, click "**Show All**" and move the cursor along the Z-stack to check that image per image, all cysts have been counted (**Supplementary Figure 8**).

2.3.3. Once new cysts have been counted and ROIs added on step 2.3.1., select the ROI set and save it via the ROI Manager window by clicking **More | Save** (**Supplementary Figure 9**).

2.3.4. Select all ROIs in the ROI Manager and click "**Measure**" in the ROI Manager to get the size of each cyst. This will open a new window of measurements named "**Results**" numbering each cyst and its estimated size. Then save in .csv format by clicking on the "**Results**" window and via the menu: **File | Save As** (**Supplementary Figure 10**).

NOTE: A macro can be created to semi-automatically process stacks, estimate cyst number/sizes from the projections, and store the data for faster counting procedure. To do so, select the tool "**Record**" in the bar menu, by clicking **Plugins | Macros | Record**.

2.4. Quantification of cyst formation efficiency

2.4.1. Count the number of cysts at day Y, ($N_{\text{cysts at day Y}}$) on a projection (Y=1, 2, 4, 7 or 10).

2.4.2. To calculate the cyst formation efficiency for 1000 cells at day Y, divide the number of cysts counted at that time point by the number of cells seeded at day 0 inferred from the hydrogel volume and multiply by 1000 (**Figure 3C, Figure 4**).

$$\text{cyst formation efficiency} = \frac{N_{\text{cysts at day Y}}}{N_{\text{cells at day 0}}} \times 1000$$

3. Cell viability

3.1. Prepare a stock solution of fluorescein diacetate (FDA) at 5 mg/mL by dissolving 5 mg of FDA in 1 mL acetone and store at -20 °C.

3.2. Prepare a stock solution of propidium iodide (PI) at a concentration of 2 mg/mL in deionized water (dH_2O) and store at 4 °C.

3.3. Prepare NRC medium without fetal calf serum (FCS).

3.4. To prepare the FDA/PI staining solution, add 4 µL of FDA stock solution (8 µg/mL final concentration) and 25 µL of PI stock solution (20 µg/mL final concentration) into 2.5 mL of NRC medium without FCS.

3.5. Remove the medium from the chamber slide, add 250 µL of staining solution into each well and incubate 4-5 min in the dark at 37 °C, 5% CO_2. Pipette out the staining solution carefully and wash once with 250 µL of 1x PBS.

3.6. Carefully add 250 µL of complete NRC medium to each well and take pictures using an inverted fluorescence microscope with Texas red and fluorescein isothiocyanate (FITC) filters. Live cells will be green and dead cells will be red (**Figure 5A**).

NOTE: In order to quantify live/dead cells, take Z-stacks across the hydrogel volume following step 2 to adapt the image processing method for fluorescence.

4. Secretion activity

NOTE: The secretion activity through the apical membrane of the cholangiocytes is assessed by the secretion of fluorescein in the lumen. Its specificity can be evaluated by doing the same test with Verapamil, a multi-drug resistant (MDR) transporter inhibitor[24].

4.1. To prepare a staining solution of Hoechst 33258 at 5 µg/mL, add 0.83 µL of Hoechst stock solution (15 mg/mL stock concentration in dH_2O) in 2.5 mL of NRC medium without FCS.

4.2. Add 250 µL of Hoechst solution in each well and incubate at 37 °C, 5% CO_2 for 15 min.

4.3. Remove the Hoechst solution and add 250 µL of FDA solution (8 µg/mL final concentration) in each well. Incubate 4-5 min at 37 °C, 5% CO_2.

NOTE: As soon as cells are exposed to FDA staining solution, the follow up of fluorescein secretion kinetics might be useful to calibrate the time needed for cysts to secrete. To do so, take pictures every min for 1 h via time-lapse imaging. In this example, the time needed to observe NRC secreting cysts in the hydrogel is about 15-20 min.

4.4. Take images using an inverted fluorescence microscope 5 min after rinsing with medium without FCS. Use 4',6-diamidino-2-phenylindole (DAPI) and FITC filters to reveal nuclei labeling and fluorescein accumulation in the lumen (**Figure 6A**). To quantify the number of secreting cysts, take Z-stacks as in step 2 and adapt the image processing steps to fluorescent images.

NOTE: For the Verapamil test, precede the previous process (steps 4.3. to 4.4.) by an incubation with Verapamil, according to the following conditions:

4.5. Prepare a stock solution of 10 mM Verapamil in dimethyl sulfoxide (DMSO). To prepare 10 µM working solution, mix 2.5 µL of Verapamil stock solution with 2.5 mL culture medium without FCS.

4.6. To assess that the fluorescence in the lumen results from MDR secretion, take another slide and add 250 µL of Verapamil working solution in each well and incubate 20 min at 37° C, 5% CO_2

4.7. Remove the solution and add 250 µL of FDA solution (8 µg/mL final concentration) into each well. Incubate 4-5 min in the dark at 37 °C, 5% CO_2. Then, wash with 250 µL of 1x PBS, before imaging (**Figure 6B, C**).

5. Epithelial polarity assessment by immunofluorescence

5.1. To prepare the fixing solution, mix 4% formaldehyde with 5% sucrose, in 1x PBS, pH 7.4 and incubate in a water bath pre-heated at 37 °C.

5.2. To fix the cells, gently pipette out the culture medium from the well without damaging the matrix. Slowly add 400 µL of the fixing solution to the side of the wells. Incubate for 20 min at room temperature (RT).

NOTE: Always leave 25 µL of the liquid above the matrix to prevent its damage.

5.3. Gently remove the fixing solution and wash 3x with 400 µL of 1x PBS at (RT).

5.4. Pipette out the PBS, add 400 µL of permeabilization solution (0.5% Triton X-100 in 1x PBS) and incubate 10 min at RT.

5.5. Gently remove the permeabilization solution, followed by 3 quick washes with 400 µL of 1x

PBS and a long washing step of 30 min at RT.

NOTE: At this step, the slide can be stored at 4 °C for 2 days. In this case, seal the slide with a paraffin film to prevent evaporation and matrix drying.

5.6. Remove the PBS, add 400 µL of blocking solution containing 0.1% bovine serum albumin (BSA) and 10% goat serum in 1x PBS and incubate for 60 min at RT.

CAUTION: Concentrations of BSA higher than 0.1% will result in lumen retraction and further cyst collapse (see **Representative Results** section) (**Figure 7A**).

5.7. Pipette out the blocking solution and wash once with 400 µL of PBS/0.05% Tween 20 and discard.

5.8. Add 150 µL of the antibody solution, e.g., E-cadherin antibody diluted 1:400 and Phalloidin 568 (16.2 nM final concentration) in 1x PBS and incubate for 90 min at RT.

NOTE: This dilution of E-cadherin is the same used as in a standard 2D immunofluorescence protocol.

5.9. Wash the sample with 400 µL of PBS/0.05% Tween 20, 3x; each time incubating the sample for 10 min at RT.

5.10. Add 150 µL of the secondary antibody (goat anti-rabbit IgG Alexa Fluor Plus 647), diluted 1:500 in 1x PBS and incubate 60 min at RT.

5.11. Wash 3x with 400 µL of PBS/0.05% Tween 20, each time incubating the sample for 10 min at RT.

5.12. Wash 3x with 400 µL of 1x PBS, each time incubating the sample for 10 min at RT.

5.13. Discard the PBS of the last wash and prepare the chamber slide for visualization via confocal microscopy following one of the two options below.

5.13.1. Add 400 µL of 1x PBS and 50 µL of DAPI per well. The samples can be examined through the bottom of the well without the need of mounting with a coverslip (**Figure 7B**).

5.13.2. Add 100 µL per well of antifade reagent containing DAPI and let the slide drying O/N at RT.

REPRESENTATIVE RESULTS:

Formation and characterization of cysts

3D cell culture systems are an important tool to study organogenesis and disease modeling[25].

Unfortunately, most of these methods are qualitative or use internal quantification performed on a single plane by comparing the number of cysts versus non-cysts, in variable and often unspecified volumes, preventing any comparison in terms of cyst formation efficiency between the various studies[7-10,15,18,23]. The method proposed in this protocol, by recording the whole number of cysts and their respective sizes over the time of the experiment, allows for the analysis of the evolution of cyst formation and growth (**Figure 4**).

Based on phase contrast images, on day 0, 8 hours after cell seeding mostly small cell aggregates are found embedded into the hydrogel. On day 1, small cysts of median diameter of 42.95 (26.53, 50.47) (first, third quartile) µm and fusion of cysts scattered throughout the hydrogel are noticeable. By day 4, it is common to observe aggregate structures as well as cysts of median diameter of 75 (56.48, 97.97) µm. By days 7 and 10 the median cyst diameter reached 108.67 (75.31, 141.76) µm and 186.46 (113.98, 278.29) µm, respectively (**Figure 4A-C**). Interestingly, the cyst formation efficiency increases from 70.03 ± 5.05 cysts/1000 cells on day 1 to 99.83 ± 12.81 cysts/1000 cells on day 4 remaining constant till day 10 (**Figure 4B**), suggesting that cysts form essentially from cell aggregates that are present at the time of the embedding or that form during the next 48h, through cell migration or the fusion of small cell aggregates. With regards to the cyst size evolution, while the mean size follows a slow and regular slope, the size distribution increases widely along the culture time, illustrating that the various cysts do not grow at the same speed. Interestingly, this can be linked to our observation (not shown) that cysts are not evenly distributed in the hydrogel, the biggest cysts lying in the center of the hydrogel volume. Since the increase of the cyst diameter mainly relies on the secretion activity (since the cell division rate is limited in NRC derived cysts), it can be inferred that this activity is highly dependent on the hydrogel properties that are not homogenous in the cell culture volume.

We then confirmed the viability of cells after embedding them into the hydrogel (day 0) and cysts on day 10 using FDA/PI live staining (**Figure 5A**). FDA is a non-fluorescent molecule that only live cells, through an enzymatic reaction, are able to convert to the green fluorescent compound fluorescein[26]. PI is a non-permeant molecule for live cells that intercalates in the DNA of necrotic cells[27]. Interestingly, dead cells that represent less than 3% of the whole cells in the culture volume at day 10, are mostly found outside the cysts, as isolated cells or part of small aggregates. However, we noticed that debris from necrotic cells accumulate in some large cysts at day 10 **(Figure 5B).** Therefore, for the maintenance of cystic cultures, passaging of cysts is recommended before 10 days in those conditions.

Functional assessment

In physiological conditions, the main function of cholangiocytes is to modify canalicular bile via absorptive and secretory mechanisms of which the MDR channel is a key player[28]. To assess the functionality of cysts, we incubated day 10 cysts with FDA/Hoechst and observed formation of fluorescein and its secretion from the basal into the apical luminal space (**Figure 6A,B**). Thus, confirming that NRCs in cysts retain their secretory functions. Moreover, the secretion of fluorescein was inhibited by pre-treatment of cysts with the MDR inhibitor Verapamil (**Figure 6C**), showing that the accumulation of fluorescence FDA into the lumen was due to the secretion through MDR transporter and not by leaking from the intercellular space.

Assessment of cyst polarity

In order to establish polarization of the NRC cysts, we conducted a series of optimization steps in the immunofluorescence protocol. One main hindering in the examination of epithelial cell polarity in the cysts is the frequent collapse of the organoid architecture during the immunofluorescence process, due to the leakage of the fluid contained in the lumen. To circumvent this problem, each step of the immunofluorescence protocol has been evaluated by testing how various conditions might affect the maintenance of cyst structure. We found that modulating the fixing (formaldehyde (2-4%) + sucrose (5-10%)) or permeabilization conditions (0.1-1% of both Triton X-100 and sucrose) did not have much impact on the cyst architecture. These ranges can be used to strongly fix and gently permeabilize the cholangiocytes (**Figure 7A**). However, we observed that keeping BSA at 0.1% or less during saturation is a key step in maintaining cyst integrity, as higher concentrations result in cyst retraction and lumen collapse (**Figure 7A**).

Cholangiocyte functions are dependent on their proper apico-basolateral polarity[29]. To verify that the NRC cysts self-assemble in hydrogel as polarized structures, we confirmed the apical and basolateral localization of F-actin and E-cadherin, respectively. E-cadherin expression in our cysts also indicates that NRCs maintain their epithelial phenotype in hydrogel (**Figure 7B**) during at least 10 days.

FIGURE AND TABLE LEGENDS:

Figure 1: Experimental workflow of cyst formation and characterization. (**A**) Hydrogel coating of the chamber slide. (**B**) Cell embedding in the hydrogel. (**C**) Microscopy of cyst formation. (**D**) A 10-day follow up assessment of cyst growth, viability, functionality, and polarization.

Figure 2: Image acquisition method. (**A**) Workflow of the Z-stack acquisition performed along the hydrogel depth from day 1 to 10: Z-stack acquisition (**1**) image processing of the Z-stack (**2**) generation of a minimum intensity projection and cyst quantification (**3**). (**B**) Image acquisition software screenshots showing the selection of the objective (**1**), the adjustment of parameters (**2**), the automatic saving of images (**3**), and the Z-stack calibration (**4**).

Figure 3: Method for the quantification of cyst size and cyst formation efficiency. (**A**) Image processing layout depicting: Z-stacks to analyze (**1**), its minimum intensity Z-projection (**2**), the final Z-projection after background subtraction (**3**) used for cyst counting and cyst size estimation. (**B**) Cyst identification on the projection (**A3**) with a zoom of the projection (**4**) to show the identification of cysts featured by a dark cell shell enclosing a brighter lumen, which are distinguished by blue lines plotted for diameter measurement vs aggregates with a dark and irregular appearance pointed by red arrows. (**C**) The formula for calculation of cyst formation efficiency for 1,000 cells.

Figure 4: Cyst formation efficiency and cyst size distribution in the hydrogel. (**A**) Time-lapse showing representative phase contrast images at days 0, 1, 2, 4, 7, and 10 of the 3D cultures. (**B**)

Plot graph with the kinetics of mean cyst formation efficiency ± SEM (n=3). (**C**) Box and whisker plot showing the cyst size distribution over the time of culture. Black bars represent the first quartile, the median and the third quartile; lines represent the width of the distribution; black dots represent the minimum and the maximum of the distribution, n=3.

Figure 5: Viability of NRC cysts in the hydrogel. (**A**) Representative fluorescent live images of cultures at day 0 and at day 10, stained with FDA (green=live) and PI (red=dead). Note that the red fluorescence was mainly associated to single cells. (**B**) Representative fluorescent live image of a necrotic cyst at day 10, where the dead cells (in red) were seen accumulating in the lumen.

Figure 6: Functionality of NRC cysts in the hydrogel. (**A**) Representative fluorescent live images of a 10-day cyst where the cell's layer was revealed by nuclei labeling with Hoechst (blue) and the lumen by the secreted FDA (green). (**B**) Representative phase contrast/fluorescent live images after a secretion test with FDA, which was shown accumulated in the lumen. (**C**) After the exposition to Verapamil, an MDR inhibitor, representative phase contrast/fluorescent live images of cysts showing that FDA was retained in the cell's layer.

Figure 7: Immunofluorescence of NRC cysts in the hydrogel. (**A**) Optimization of the immunofluorescence protocol with bright field images showing representative cyst shapes at each step of the protocol. From left to right: (**Living cyst**) a live cyst in complete medium before fixation, (**Fixation**) a cyst after fixation, (**Permeabilization**) another cyst after permeabilization, (**Saturation**) a cyst after the saturation step and (**Labeling**) a cyst at the immunolabeling step. (**B**) (1-2): Confocal images of a section through a cyst showing the apical surface marker F-actin (red-orange), the basolateral marker E-cadherin (green) and the nuclei stained with DAPI (blue). (3): 3D reconstitution of a set of cysts with the following labelings: red-orange for F-actin and green for E-cadherin.

Supplementary Figure 1: Opening of a stack. Screenshot captures of the software depicting the procedure to open a Z-stack.

Supplementary Figure 2: Stack duplication. Screenshot captures of the software showing the process to duplicate a Z-stack.

Supplementary Figure 3: Generation of a minimum intensity projection. Screenshot captures of the software illustrating the procedure to create a minimum intensity projection from the duplicated Z-stack.

Supplementary Figure 4: Background removal. Screenshot captures of the software portraying the method to remove the background from the Z-stack projection.

Supplementary Figure 5: Contrast enhancement. Screenshot captures of the software outlining the steps to enhance the contrast of the Z-stack projection.

Supplementary Figure 6: Picture calibration. Screenshot captures of the software delineating the process to calibrate the Z-stack and the Z-stack projection in microns.

Supplementary Figure 7: Cyst counting. Screenshot captures of the software depicting the procedure to count cysts on the Z-stack projection with the straight-line tool.

Supplementary Figure 8: Cyst counting check-up. Screenshot captures of the software outlining the method to compare the number of cysts counted on the Z-stack projection and the Z-stack.

Supplementary Figure 9: ROI saving. Screenshot captures of the software showing how to save the ROI set defined by the countings.

Supplementary Figure 10: Cyst size and number measurements. Screenshot captures of the software detailing how to measure and save cyst size and cyst number from the Z-stack projection and the Z-stack.

DISCUSSION:

In order to study organogenesis and maintenance of 3D cellular structures, various tissues have been modelled, using different cellular origins but also different types of extra-cellular matrices including synthetic hydrogels[8-10,21]. However, due to lack of 3D quantitative analysis that allows for comparisons between methods in terms of organoids formation or functionality[7-10,15,18], further standardization for hydrogel or drug screening remains out of reach.

To address these deficiencies, we propose a hydrogel-based, reproducible, and standardized protocol to generate epithelial cell-derived cysts. Here, we exemplified it with the formation of biliary cysts in a basal lamina derived hydrogel, from a referenced cholangiocyte cell line. To unlock the limitation of 3D quantification, cyst formation efficiency is calculated relative to the total number of cells seeded into the hydrogel and cyst growth kinetics is measured across a constant hydrogel volume.

We provide a series of systematic steps to generate and characterize cysts, to allow relevant cyst quantitative analysis. To this aim, special efforts have been made to generate a uniform distribution of cell aggregates at the time of hydrogel embedding and circumvent the heterogeneity of the hydrogel's structure, which impacts cyst formation by setting the conditions to have a representative sample for cyst counting.

Experimental reproducibility is addressed through critical steps such as, filtering cell suspensions to limit cell aggregate size and pre-coating of the chamber slides prior to cell-hydrogel addition to avoid 2D layer formation when cells contact the surface of the culture vessel. Consistent quantification is solved taking pictures along the Z-axis of the hydrogel with a constant set of parameters across different samples and experiments.

Cyst formation efficiency and cyst growth kinetics are estimated from the total number of cells seeded into the hydrogel. Consequently, an adaptable algorithm for image processing is

proposed to segment images for cyst counting and cyst size measurements. The novelty of the method proposed is that the counting and measurements are done on Z-stack projections. After removal of the specific background, the number of images to analyze is restricted, allowing for a considerable gain of time and limiting hard disk's saturation. Immunofluorescence is a significant tool to analyze 3D cultures at the structural level, in particular polarization, key in proper epithelial cell function[4]. Thus, we undertook the task to carefully optimize the fixation, permeabilization, and blocking steps of the immunofluorescence part of our protocol; troubleshooting BSA concentration to prevent cyst retraction and further lumen collapse.

Altogether the method proposed opens the pathway to generate a simple, reproducible, and costly-effective protocol, 3D cellular cultures and investigate qualitative and quantitative parameters. Furthermore, this method allows for comparisons between different types of matrices: using the same method with poly(ethylene glycol) (PEG)-derived hydrogels we could demonstrate that lumen formation and growth are critically dependent on the hydrogel stiffness and adhesiveness, respectively[21]. This protocol is also applicable for comparing formation and function of spheroids derived from different cells, which could participate to the standardization of tissue-specific epithelial spheroid models. However, a limitation is that the optimization of culture conditions such as culture media, initial cell seeding, and the time needed for cyst formation might be required for other cell types. In the bile duct field, this work might contribute to answer questions regarding bile duct organogenesis, as well as molecular pathways of disease, and drug testing. This protocol will also find its limit when applied to high throughput analysis since some steps like cyst counting and imaging processing are not automatized yet, even though we propose macros for semi-automatizing the imaging process that could be further developed for automatization. The limitation to automatic processing in this case is the image background. This is due to heterogeneous structure of natural complex hydrogels such basement membrane type gels, but we believe that automatization might be applied to transparent gels such as PEG-derived hydrogels.

ACKNOWLEDGMENTS:

We thank Dr. Nicholas LaRusso (Mayo Clinic, Rochester, Minnesota, United States), who kindly provided the NRC cell line.

This work received the financial support of both the iLite RHU program (grant ANR-16-RHUS-0005) and the DHU Hepatinov.

We thank Isabelle Garcin and Réseau d'Imagerie Cellulaire Paris Saclay for their support on imaging.

DISCLOSURES:

The authors have nothing to disclose.

REFERENCES:

1 Edmondson, R., Broglie, J. J., Adcock, F., Yang, L. Three-Dimensional Cell Culture Systems and Their Applications in Drug Discovery and Cell-Based Biosensors. *ASSAY and Drug Development Technologies.* **12** (4), 207-218 (2014).

2 Martín-Belmonte, F. et al. Cell-polarity dynamics controls the mechanism of lumen formation in epithelial morphogenesis. *Current Biology.* **18**, 507-513 (2008).
3 Debnath, J., Muthuswamy, S. K., Brugge, J. Morphogenesis and oncogenesis of MCF-10A mammary epithelial acini grown in three-dimensional basement membrane cultures. *Methods.* **30** (3), 256-268 (2003).
4 Artym, V. V., Matsumoto, K. Imaging Cells in Three-Dimensional Collagen Matrix. *Current Procotols in Cell Biology.* **Chapter 10** (Unit 10) (2010).
5 Petersen, O. W., Ronnov-Jessen, L., Howlett, A. R., Bisell, M. J. Interaction with basement membrane serves to rapidly distinguish growth and differentiation pattern of normal and malignant human breast epithelial cells. *Proceedings of the National Academy of Sciences of the United States of America.* **89**, 9064-9068 (1992).
6 Kim, S. P., Lee, D. H., Park, J. K. Development of hepatocyte spheroids immobilization technique using alternative encapsulation method. *Biotechnology and Bioprocess Engineering.* **3**, 96-102 (1998).
7 Lorent, K. et al. Identification of a plant isoflavonoid that causes biliary atresia. *Science Translational Medicine.* **7** (286) 286ra67, (2015).
8 Nowak, M., Freudenberga, U.,Tsurkana, M. V., Wernera, C., Levental, K.R. Modular GAG-matrices to promote mammary epithelial morphogenesis *in vitro*. *Biomaterials.* **112,** 20-30 (2017).
9 Miroshnikova, Y. A. et al. Engineering Strategies to Recapitulate Epithelial Morphogenesis Within Synthetic Three-Dimensional Extracellular Matrix With Tunable Mechanical Properties *Physical Biology.* **8** (2), 026013 (2011).
10 Ozdemir, T. et al. Tuning Hydrogel Properties to Promote the Assembly of Salivary Gland Spheroids in 3D. *ACS Biomaterials Science & Engineering.* **2** (12), 2217-2230 (2016).
11 Dolega, M. E., Abeille, F., Picollet-D'hahan, N., Gidrol, X. Controlled 3D culture in Matrigel microbeads to analyze clonal acinar development. *Biomaterials.* **52,** 347-357 (2015).
12 Laperrousaz, B. et al. Direct transfection of clonal organoids in Matrigel microbeads: a promising approach toward organoid-based genetic screens. *Nucleic Acids Research.* **46** (12), e70 (2018).
13 Lazaridis, K. N., LaRusso, N. F. The Cholangiopathies. *Mayo Clinic Proceedings.* **90** (6), 791-800 (2015).
14 Tam, P. K., Yiua, R. S., Lendahl, U., and Andersson, E.R. Cholangiopathies – Towards a molecular understanding *EBioMedicine.* **35**, 381-393 (2018).
15 Loarca, L. et al. Development and characterization of cholangioids from normal and diseased human cholangiocytes as an *in vitro* model to study primary sclerosing cholangitis *Laboratory Investigation.* **97**, 1385-1396 (2017).
16 De Assuncao, T. M., Jalan-Sakrikar, N., Huebert, R. C. Regenerative medicine and the biliary tree. *Seminars in Liver Disease.* **37,** 17-27 (2017).
17 Dianat, N. H. et al. Generation of functional cholangiocyte-like cells from human pluripotent stem cells and HepaRG cells. *Hepatology.* **60**, 700-714 (2014).
18 Masyuk, A. I. et al. Cholangiocyte autophagy contributes to hepatic cystogenesis in polycystic liver disease and represents a potential therapeutic target. *Hepatology.* **67** (3), 1088-1108 (2018).
19 Sampaziotis, F., Cardoso, M., Madrigal, P., Bertero, A., Saeb-Parsy, K., *et al.*

Cholangiocytes derived from human induced pluripotent stem cells for disease modeling and drug validation. *Nature Biotechnology.* **33** (8), 845–852 (2015).

20 Soroka, J. C. et al. Bile-Derived Organoids From Patients With Primary Sclerosing Cholangitis Recapitulate Their Inflammatory Immune Profile. *Hepatology.* **70** (3), 871-882 (2019).

21 Funfak, F. et al. Biophysical Control of Bile Duct Epithelial Morphogenesis in Natural and Synthetic Scaffolds. *Frontiers in Bioengineering and Biotechnology.* **7** (417), 417 (2019).

22 Du, Y. et al. A Bile Duct-on-a-Chip With Organ-Level Functions. *Hepatology.* **0** (0), (2019).

23 Shiota, J. M., Mohamad Zaki N. H., Merchant, J. L., Samuelson, L. C., Razumilava, N. Generation of Organoids from Mouse Extrahepatic Bile Ducts. *Journal of Visualized Experiments.* (146), e59544 (2019).

24 Bircsak, K. M., Richardson, J. R., Aleksunes, L.M. Inhibition of Human MDR1 and BCRP Transporter ATPase Activity by Organochlorine and Pyrethroid Insecticides. *Journal of Biochemical and Molecular Toxicology.* **27** (2), 157-164 (2013).

25 Fennema, E., Rivron, N., Rouwkema, J., Blitterswijk, C., Boer, J. Spheroid culture as a tool for creating 3D complex tissues. *Trends in Biotechnology.* **31** (2), 108-115 (2013).

26 Kanade, S., Nataraj, G., Ubale, M., Mehta, P. Fluorescein Diacetate Vital Staining for Detecting Viability of Acid-Fast Bacilli in Patients on Antituberculosis Treatment. *International Journal of Mycobacteriology.* **5** (3), 294-298 (2016).

27 Rieger, A. M., Nelson, K. L., Konowalchuk, J. D., Barreda, D. R. Modified Annexin V/Propidium Iodide Apoptosis Assay For Accurate Assessment of Cell Death. *Journal of Visualized Experiments.* **50**, e2597, (2011).

28 Tabibian, J. H., Masyuk, A., Masyuk, T. V., O'Hara, S. P., LaRusso, N. F. Physiology of Cholangiocytes. *Comprehensive Physiology.* **3** (1), 10.1002/cphy.c120019. (2013).

29 Spirlì, C. et al. Functional polarity of Na^+/H^+ and Cl^-/HCO_3^- exchangers in a rat cholangiocyte cell line. *American Journal Physiology.* **275**, G1236-G1245 (1998).

Figure 1

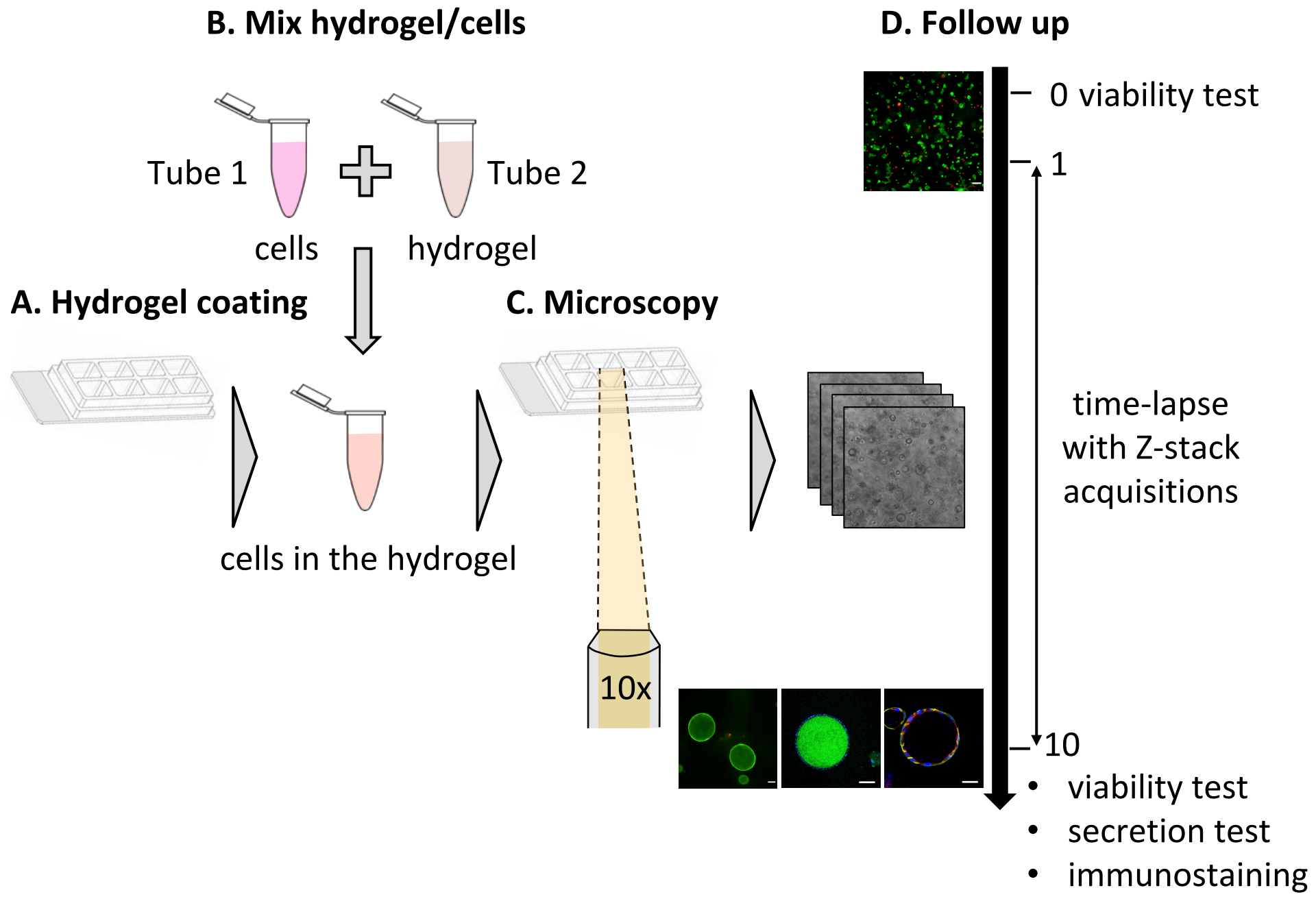

Figure 2 **A. Workflow**

day 1 to 10:

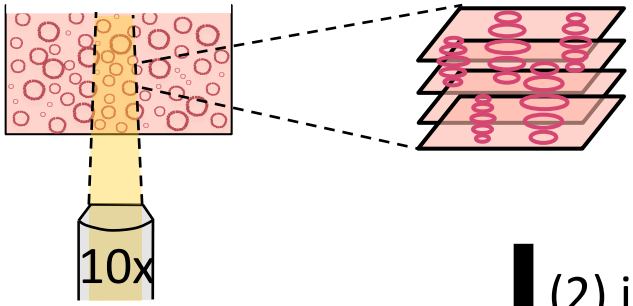

(1) Z-stacks acquisition

(2) image processing

minimum intensity projection (3)

B. Image acquisition software

(1)

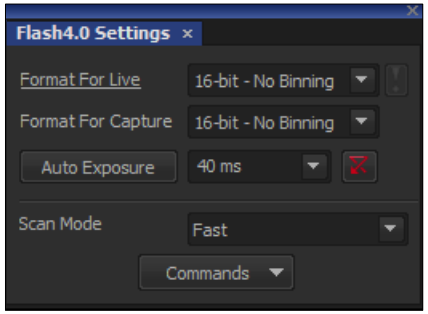

(2)

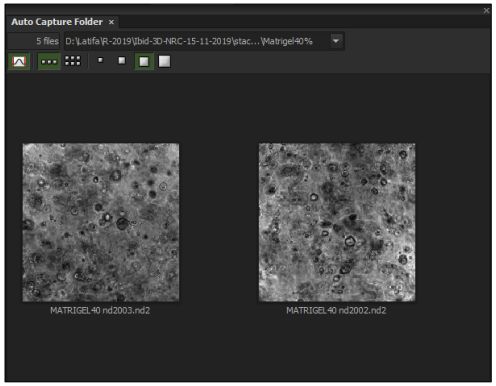

(3)

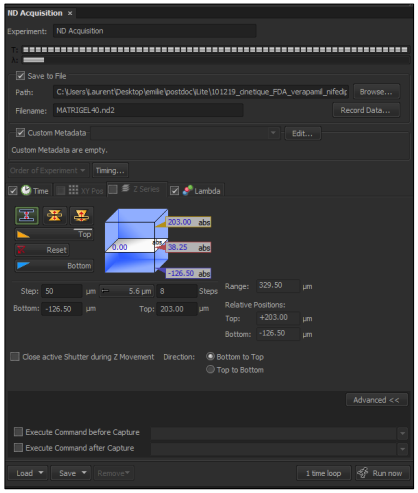

(4)

Figure 3

A. Image processing

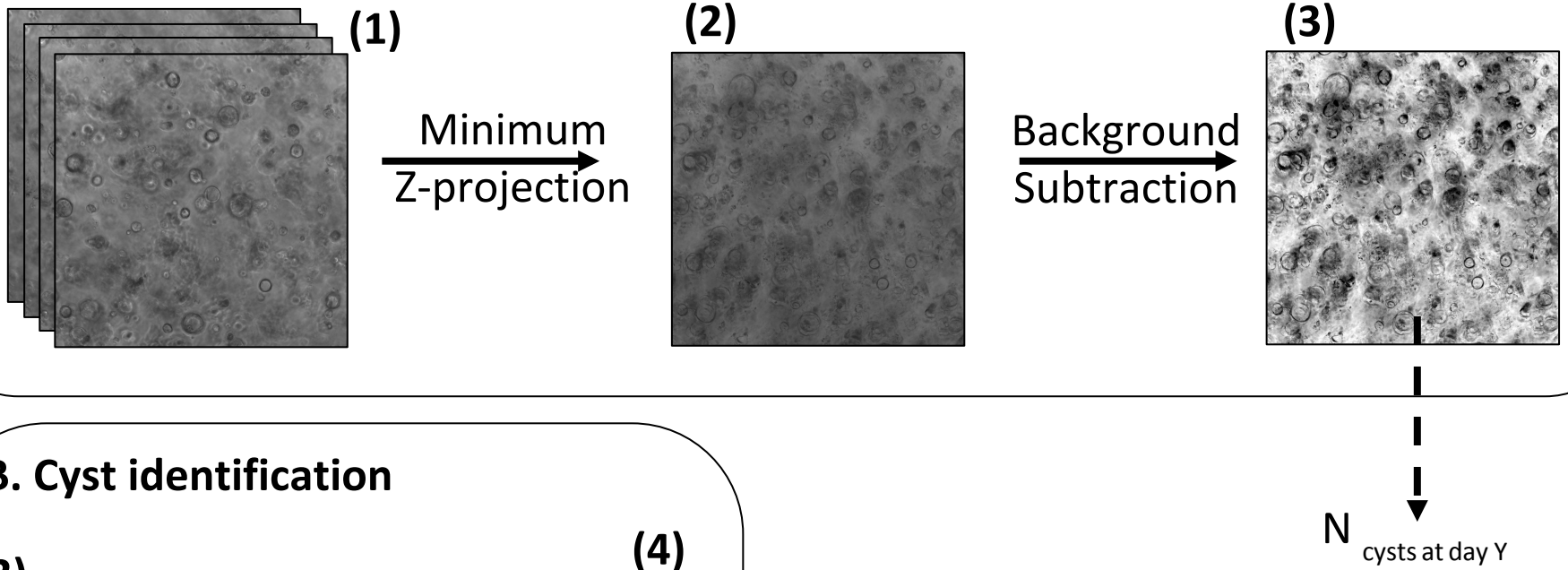

B. Cyst identification

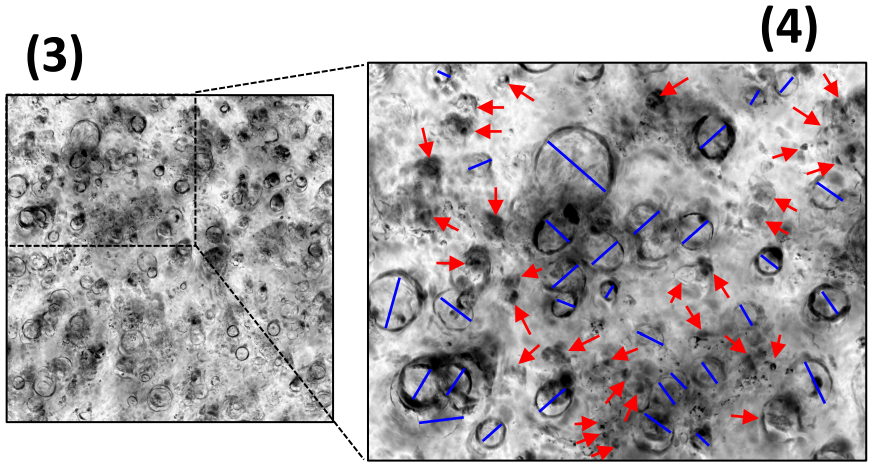

C. Cyst formation efficiency

$$\text{cyst formation efficiency} = \frac{N_{\text{cysts at day Y}}}{N_{\text{cells at day 0}}} \times 1000$$

$$Y = \{1, 2, 4, 7, 10\}$$

Figure 4

Click here to access/download;Figure;Figure4_high_2.ai

A. Time-lapse

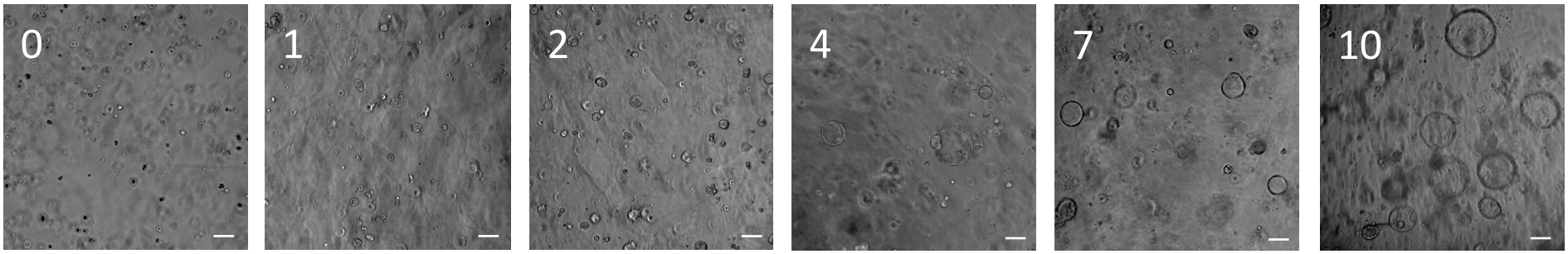

B. Cyst formation efficiency

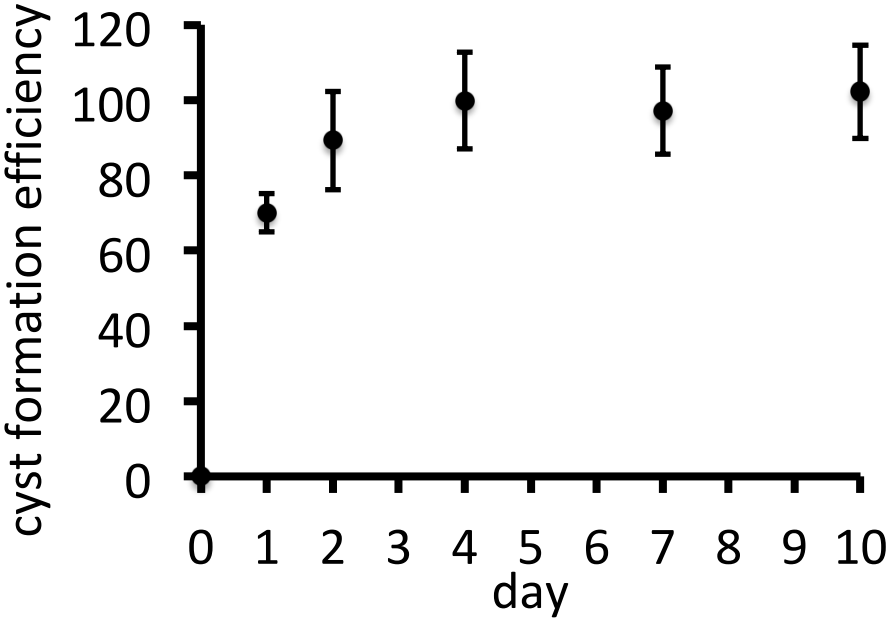

C. Cyst size distribution

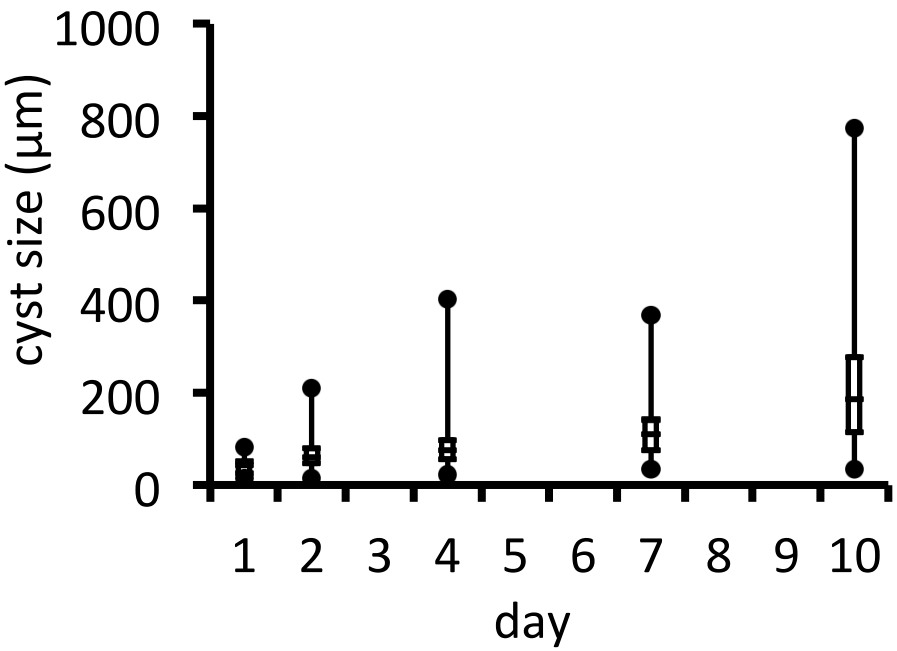

Figure 5

A. Live/dead cells images

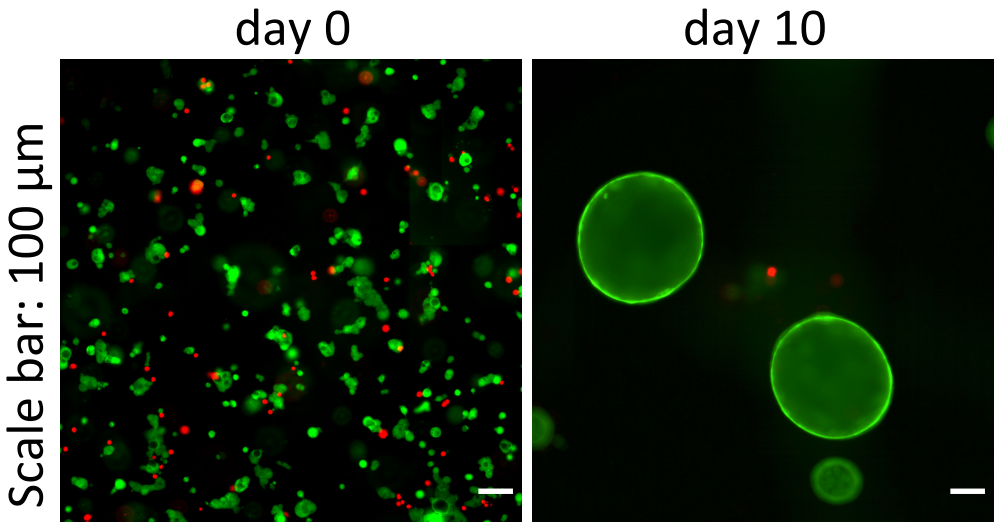

B. Necrotic cyst at day 10

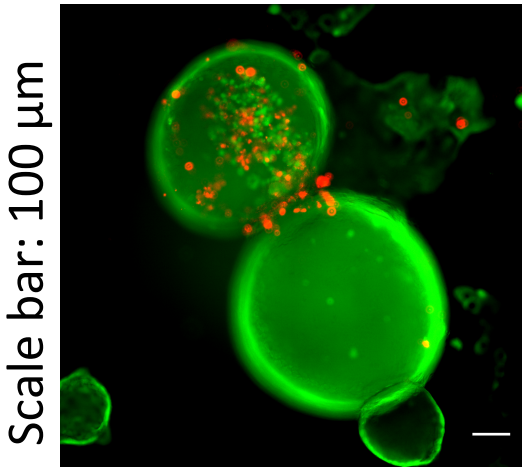

FDA: living cells

PI: dead cells

Figure 6

Click here to access/download;Figure;Figure6_high_2.ai

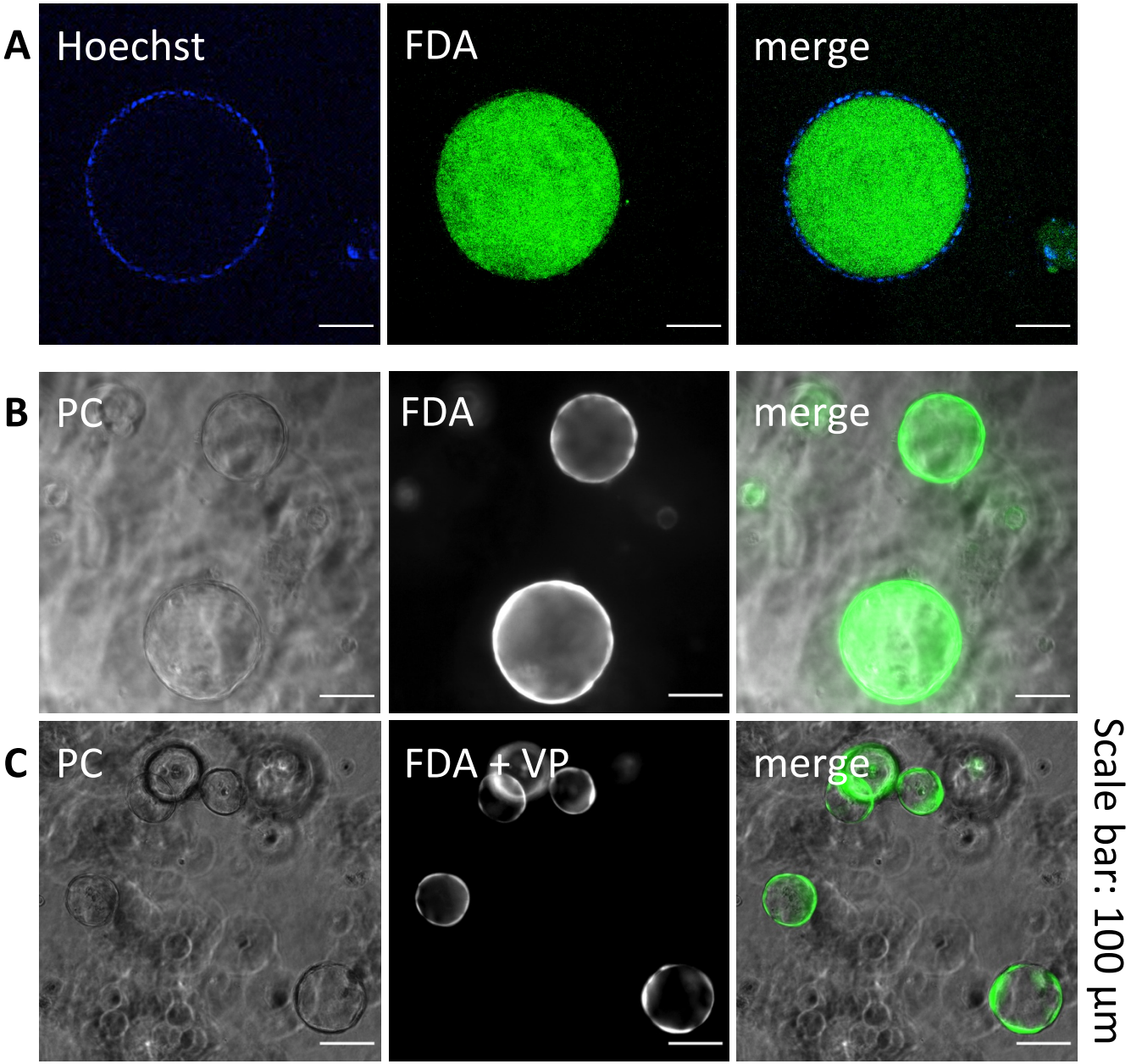

Figure 7

Click here to access/download;Figure;Figure7_high_2.ai

A. Optimization of the immunofluorescence protocol

Scale bar: 200 µm

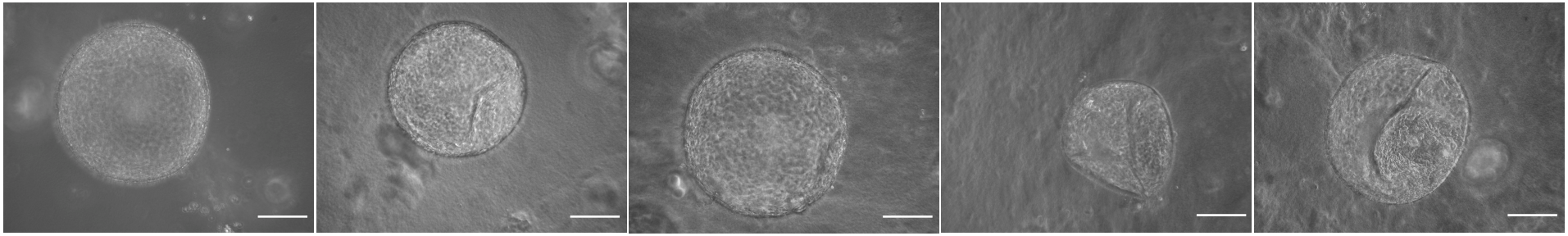

Living cyst | Fixation | Permeabilization | Saturation | Labeling

B. Apico-basal polarity

Scale bar: 100 µm

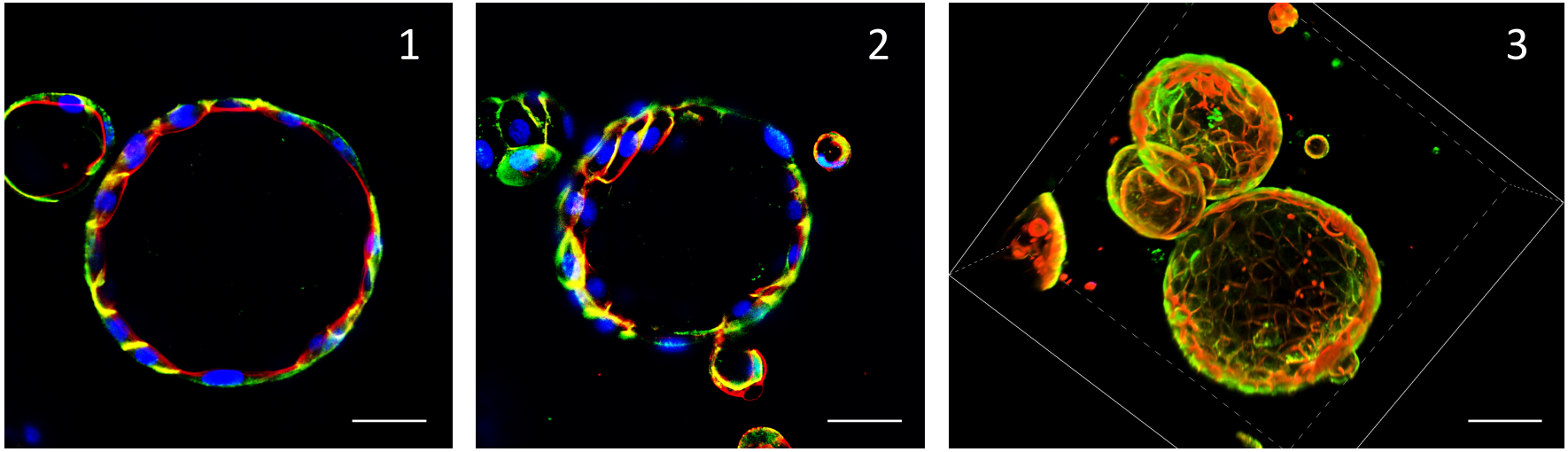

Table of Materials

Name of Material/ Equipment	Company	Catalog Number	Comments/Description	NRC complete medium final concentration
10 µl- Pipette Eppendorf Research Plus	Thermo Fisher Scientific	3120000020		
100 µl - Pipette Eppendorf Research Plus	Thermo Fisher Scientific	3120000046		
1000 µl - Pipette Eppendorf Research Plus	Thermo Fisher Scientific	3120000062		
1X PBS	Thermo Fisher Scientific	14190-094		
200 µl - Pipette Eppendorf Research Plus	Thermo Fisher Scientific	3120000054		
3,3',5-Triiodo-L-thyronine sodium salt	Sigma-Aldrich	T5516		3.4 µg/mL
Acetic acid	VWR	20104-298	0.02N final	
Aerosol barrier pipettes tips 10 µl (Fisherbrand)	Thermo Fisher Scientific	2707439		
Aerosol barrier pipettes tips 1000 µl (Fisherbrand)	Thermo Fisher Scientific	2707404		
Aerosol barrier pipettes tips 200 µl (Fisherbrand)	Thermo Fisher Scientific	2707430		
Antibiotic Antimicotic Solution (100X)	Sigma-Aldrich	A5955		1:100 dilution
Bovine pituitary extract	Thermo Fisher Scientific	13028-014		30 µg/mL
Bovine serum albumin	Sigma-Aldrich	A2153	1:1000 dilution	
Chemically Defined Lipid Concentrate (100X)	Thermo Fisher Scientific	11905-031		1:100 dilution
Collagen high concentration, rat tail	Thermo Fisher Scientific	354249	50 µg/mL final concentration	
Dexamethasone	Sigma-Aldrich	D4902		0.393 µg/mL
DMEM F12	Thermo Fisher Scientific	21331-020		1X
E-cadherin Rabbit anti-Human, Rat, Polyclonal	Thermo Fisher Scientific	PA5-32178	1:400 dilution	
Eclipse TE300 inverted microscope	Nikon		imaging	
Ethanolamine	Sigma-Aldrich	E9508		0.32 mM
Fetal calf serum	Thermo Fisher Scientific	10270-106		5:100 dilution
Fluoroshield with DAPI (Mounting medium)	Sigma-Aldrich	F6057		
Formaldehyde 16% (W/V)	Thermo Fisher Scientific	28906	4% (W/V)	
Goat serum	Thermo Fisher Scientific	16210-064	1:10 dilution	
Hamamatsu camera (Digital camera C11440 ORCA - flash 4.OLT)	Hamamatsu		imaging	
Hoechst 33258	Sigma-Aldrich	B1155	5 µg/mL final concentration	
IgG (H+L) Highly Cross-Adsorbed Goat anti-Rabbit, Alexa Fluor Plus 647	Thermo Fisher Scientific	A32733	1:500 dilution	
ImageJ version 2.0.0-rc-69/1.52n			Open source image processing software	
Insulin-Transferrin-Selenium (100X)	Thermo Fisher Scientific	51300-044		1:100 dilution
L-Glutamine (100X)	Thermo Fisher Scientific	25030-024		1:100 dilution
Matrigel GFR (stock concentration 9.7 mg/mL)	Thermo Fisher Scientific	356231	4:10 dilution	
NIS Elements software version 4.50.00	Nikon		image acquisition and display	
Non-Essential-Amino-Acids-Solution (100X)	Thermo Fisher Scientific	11140-035		1:100 dilution
Objective Plan Fluor 10X/0.30 Ph1 DL (∞/1.2 WD 15.2)	Nikon			
Prolong Gold Antifade Reagent	Thermo Fisher Scientific	P36931		
Propidium Iodide (PI)	Sigma-Aldrich	P4170	20 µg/mL final concentration	
Rhodamine Phalloidin	Thermo Fisher Scientific	R415	16.2 nM final concentration	
Sir-Actin / Verapamil kit	Spirochrome	SC001	10 µM final concentration	
Soybean trypsin inhibitor	Thermo Fisher Scientific	17075-029		50 µg/mL
Sterile cell strainer 40 µm (Fisherbrand)	Thermo Fisher Scientific	22363547		
Sterile pipettes 10 mL (Fisherbrand)	Thermo Fisher Scientific	1367811E		
Sterile pipettes 5 mL (Fisherbrand)	Thermo Fisher Scientific	1367811D		
Sterile tubes 1.5 mL (Fisherbrand)	Thermo Fisher Scientific	11926955		
Sterile tubes 15 mL (Fisherbrand)	Thermo Fisher Scientific	7200886		
Sterile tubes 50 mL (Fisherbrand)	Thermo Fisher Scientific	553913		
Sucrose	Sigma-Aldrich	S0389	5:100 dilution	
Tissue culture treated flask 25cm^2 (Falcon)	Thermo Fisher Scientific	353108		
Triton X-100	Sigma-Aldrich	T8787	5:1000 dilution	
Trypsin-EDTA (0.05%) phenol red	Thermo Fisher Scientific	25300-054	1X	
Tween-20	Sigma-Aldrich	P1379	5:10000 dilution	
Vitamin (100X)	Thermo Fisher Scientific	11120-037		1:100 dilution
µ-Slide 8 Well ibiTreat, Ibidi	Clinisciences	80826		

université
PARIS-SACLAY

April 6, 2020

Alisha DSouza, Ph.D.
Senior Review Editor
Journal of Visualized Experiments (JoVE)
1 Alewife Center, Ste, 200
Cambride, MA 02140
United States of America

Re: revised-manuscript submission

To: Alisha DSouza, Ph.D.

Dear Dr. DSouza,

We thank you and the reviewers for considering and evaluating our manuscript for publication in JoVE as an original article. Based on the editor/reviewers' comments, we are pleased to submit a revised version entitled, "A reproducible method to generate and quantitatively characterize functional and polarized biliary epithelial cysts".

We appreciate your suggestions to make our manuscript more comprehensive and have considered all the comments and modified the manuscript accordingly. All the modifications have been highlighted in blue in the revised manuscript. Below we are addressing in blue point-by-point your concerns.

Answers to the editorial comments

• Please take this opportunity to thoroughly proofread the manuscript to ensure that there are no spelling or grammatical error. The manuscript has been carefully revised and proofread and all our changes are underlined in blue.

• **Protocol Detail:** Please note that your protocol will be used to generate the script for the video, and must contain everything that you would like shown in the video**.** Please add more specific details (e.g. button clicks for software actions, numerical values for settings, etc) to your protocol steps. There should be enough detail in each step to supplement the actions seen in the video so that viewers can easily replicate the protocol.

1) 1.2.1: what is the composition of complete medium? The composition of the complete NRC medium is detailed in the **Table of Materials.**

We have added more specific details to the protocol to ensure its replicability, such as button clicks for software actions and numerical values used for contrast enhancement of processed images (see the section "2. Cyst quantification" from lines 206-321.

• **Protocol Highlight:** After you have made all of the recommended changes to your protocol (listed above), please re-evaluate the length of your protocol section. There is a 10-page limit for the protocol text, and a 3-page limit for filmable content. If your protocol is longer than 3 pages, please highlight ~2.5 pages or less of text (which includes headings and spaces) in yellow, to identify which steps should be visualized to tell the most cohesive story of your protocol steps. I suggest including some quantitative analysis steps.

1) Ensure that the highlighting best represents the title, I suggest highlighting some quantitative analysis as well.

The new highlighted part best represents the title of our manuscript and includes quantitative analysis.

2) The highlighting must include all relevant details that are required to perform the step. For example, if step 2.5 is highlighted for filming and the details of how to perform the step are given in steps 2.5.1 and 2.5.2, then the sub-steps where the details are provided must be included in the highlighting.

We have taken care of this in the new version.

3) The highlighted steps should form a cohesive narrative, that is, there must be a logical flow from one highlighted step to the next.

We took this instruction into account to select highlights representing a cohesive narrative scenario for the movie.

• **Discussion:** JoVE articles are focused on the methods and the protocol, thus the discussion should be similarly focused. Please ensure that the discussion covers the following in detail and in paragraph form (3-6 paragraphs): 1) modifications and troubleshooting, 2) limitations of the technique, 3) significance with respect to existing methods, 4) future applications and 5) critical steps within the protocol.

We thank the editor for drawing our attention on these elements. In the revised manuscript, we paid attention at covering all the significance, critical steps, troubleshooting, and future applications of our protocol.

• **Commercial Language:** JoVE is unable to publish manuscripts containing commercial sounding language, including trademark or registered trademark symbols (TM/R) and the mention of company brand names before an instrument or reagent. Examples of commercial sounding language in your manuscript are Matrigel, a Nikon Eclipse, NIS Elements,
1) Please use MS Word's find function (Ctrl+F), to locate and replace all commercial sounding language in your manuscript with generic names that are not company-specific. All commercial products should be sufficiently referenced in the table of materials/reagents. You may use the generic term followed by "(see table of materials)" to draw the readers' attention to specific commercial names.

We removed all commercial names from our manuscript and included them in the **Table of Materials.**

• Table of Materials: Sort by alphabetical order.

As suggested, we sorted the **Table of Materials** by alphabetical order.

• If your figures and tables are original and not published previously or you have already obtained figure permissions, please ignore this comment. If you are re-using figures from a previous publication, you must obtain explicit permission to re-use the figure from the previous publisher (this can be in the form of a letter from an editor or a link to the editorial policies that allows you to re-publish the figure). Please upload the text of the re-print permission (may be copied and pasted from an email/website) as a Word document to the Editorial Manager site in the "Supplemental files (as requested by JoVE)" section. Please also cite the figure appropriately in the figure legend, i.e. "This figure has been modified from [citation]."

N/A

Answers to the reviewers' comments

Reviewer #1:

Manuscript Summary:

The authors present a protocol to generate cholangiocyte cysts in a 3D hydrogel, and a methodology to quantify and characterize the cysts throughout the thickness of the gel (not restricted to a single plane), which would lead to a more objective and quantitative analysis of the characteristics of the cyst population. This would also allow to conduct comparative quantitative assays of cyst formation, varying hydrogel composition, factors, inhibitors etc. to evaluate their effect on organogenesis.

Major Concerns:

* A major concern is the instructions for the image processing methodology. (2.2 & 2.3) These are not clear enough to guide the reader/viewer and some steps can be subject to biais, in particular in identifying the real cysts from "non cysts", and all measurements are manual, not automated.

In the revised protocol we clarified many points of doubt for the quantification method and for the corresponding figures. Below, we addressed point-by-point each one of your questions/suggestions. Our changes are underlined in blue.

Please find in the Following some detailed questions and concerns for the substeps of this section.

2.2.2 Please indicate which thresholding algorithm should be used.

In the revised manuscript, we clarified the image processing method and incorporated the different algorithms used for intensity projection and background subtraction. In particular, lines 271-283 more precisely step 2.2.3., that we used a minimum intensity projection, step 2.2.4. we specify the size of the rolling ball radius used for the background subtraction (500 pixels) and we also provide step 2.2.5. contrast enhancement parameters associated to the final projection obtained and used for cyst counting.

2.2.3 It is unclear what exactly is being "substracted to the z-stack". The sentence seems to indicate that you are substracting the binary mask (made of 0 or 1) from each (grayscale) image from the Z stack. Or are you using the mask to cut each image and keep only the "black" regions on each image to recalculate a projection? Then what background are you substracting? and what is the purpose of this background substraction as no quantification of the greyscale image is carried out in the next steps.

In the image processing method presented (**Figure 3A**), the background subtraction is operated on the minimum intensity projection of the Z-stack and the final cyst counting/cyst size measurements are done on this corrected projection. The purpose of the background subtraction is to segment cyst objects, more contrasted at the level of their cell shell than the hydrogel considered as background.

2.3.1 "Mean diameter" of the cyst appears to be drawn manually as a line.

Yes, the "mean size" of each cyst is estimated manually since our resulting projections are still very noisy and it would have been difficult to automatize the detection and counting process without inducing errors. It is difficult to entirely segment cyst objects from the background (hydrogel). Even after background subtraction, we clearly see that not all the cysts have a constant gray level intensity along their shell. Thus, applying a threshold to binarize cysts would have resulted in partial cyst detection, thus ultimately leading to inaccurate size estimation.

Additionally, as cyst shells, single cells and aggregates might have the same gray levels and intensity variations, automatizing the detection process (threshold) would have resulted in error detection. However, this process is not necessary for other types of hydrogels, which do not generate such background as BME like hydrogels. Therefore, the protocol described here could be simplified and prone to automation of cyst detection.

Wouldn't it be better to fit a circle to the object?
We think that fitting a circle to the object would not be appropriate since some cysts are not completely circular. Alternatively, we think that estimating the mean size by a straight line is more adapted and more convenient when identifying around 200 cysts over the whole set of projections analyzed. Based on our calculations, the error estimation of fitting a line on a rounded cyst instead of a circle is less than 5%.

Mean diameter should be the result of a calculation over a set of values. Instead of "mean", maybe the term "approximate" diameter should be used.
We totally agree with this and therefore, we replaced the term “mean” in the manuscript by “approximate” (see line 290).

In this section, the criteria used to determine which objects are cysts should be explicited.
These criteria are given in the legend of figure 3 but these appear insufficient to determine the nature of all the objects seen in figure 3: in this respect, do you suggest that there are only 2 cysts on the projection image in A? I would suggest to add either blue or red arrows to ALL the objects of this image to guide the viewer as to which objects should be measured or not.
We modified Figure 3 in order to show without ambiguity which objects are considered as cysts (blue lines), and which ones are not considered cysts (red arrows).

Along the same reasoning, in figure 5B, the red arrow is pointing to a necrotic cyst, but according to your definition of a cyst in Figure 3, this object shouldn't be identified as a cyst.
To avoid any ambiguity we removed the phase contrast image of Figure 5B.

* Section 2.4 needs clarification
2.4.1 Line 258: "#cysts" is present on both side of the formula but mean two different things! Add a $\bar{}$ to indicate "average" over "number of cysts" and write the formula the other way round: $\bar{}$ (number of cysts)/image = number of cysts/number of images
In the new version of the manuscript, we rephrased the mathematical magnitudes and the formula to better explain how the cyst formation efficiency is calculated (see sub-sections 2.4.1 and 2.4.2 from lines 314-322).

As the same cyst is present on many successive images from the stack, it isn't clear what this "mean number of cysts per image" is supposed to represent.
We thank the reviewer for this observation. This was an error in selecting the images for the stack. So we corrected the figures 1 and 3 accordingly. The “mean number of cysts” is obtained by averaging the number of cysts on different projections for each time point.

2.4.2 How is the mean number of cells/image calculated? From the day 0 stack? It seems that cells have already aggregated at day 0. This should be clarified.
The number is calculated from the initial conditions *i.e.* the number of seeded cells and the volume of the hydrogel; the number of cells/image is inferred from the height of the stack and the corresponding hydrogel volume. The images made at D0 allow to check that cell distribution is uniform throughout the hydrogel volume.

* Generally speaking, I think it would make more sense to say that all stacks from day 0,1,..10 must contain the same number of images taken with the same z interval (therefore from an identical volume), and this z interval should be smaller than the size of a single cell (otherwise the final efficiency will be biased).
We have clarified this point by adding various notes in the section 2.1 Cyst imaging, lines 214-216
In our conditions, and according to this magnification, the depth of view allows to detect small cell aggregates and differentiate them from cysts with a Z-step of 20 µm., lines 238-241

Then the efficiency can be calculated directly from a given number of n projection images (i.e. stacks) for each timepoint. For robust quantification, a significant number of objects should be counted. This significant number should be discussed.
To be in line with this comment, we added a note in the section 2.1, where we precise the number of cysts counted for each time point, lines 250-253 Thus, we are in the ± 5% error bar for the mean cyst formation efficiency calculated each day.

Efficiency = number of cysts counted in n stack projections from day10/number of cells in n stack projections from day 0 (or x1000 if you want to represent efficiency over a 1000 cells)
We really appreciate the reviewer's help to clarify our manuscript. We hope that based on his/her suggestions, all ambiguities have been solved.

Minor Concerns:
* I would recommend changing the title of the article to better guide the reader/viewer on what they can learn in this protocol.
The title currently reads: "A QUANTITATIVE (and..) method to GENERATE (..) cysts", whereas the article explains how to QUANTIFY cyst formation EFFICIENCY
I would also add "cholangiocyte" or "biliary" to the title as the article focuses only on this example (starting off from the first sentences of the abstract) and secretion analysis is also specific to this cell model.
For example: A Reproducible method to generate and quantitatively characterize functional and polarized biliary epithelial cysts.
We changed the title of our manuscript accordingly as it best illustrates the purpose of our study.

* Multiple times (lines 39-42; 83-87; 390-392; 516-518) authors mention the lack of quantitative characterization of cyst samples in current publications. But no references are provided.
We took these remarks in consideration adding corresponding references to support our ideas.

* Lines 36-37 - what is a "growth hydrogel"? This term is unfamiliar and therefore needs to be defined.
We have removed the term "growth hydrogel" leaving it just as "hydrogel".

* In lines 46-48 it is stated that the method allows quantify cyst distribution along the vertical axis, but at the same time in chapters 2.3/2.4 it is stated that cysts' quantification is performed using Z-stack projections which excludes the possibility to follow the distribution in the various planes.
Indeed using Z-stack projections excludes the possibility to probe cyst distribution across the planes. However, to ensure the applicability of the method, we took Z-stacks in the inner part of the gel where cysts are more homogenously distributed than on the edges where hydrogel polymerization heterogeneities are too high.

* Line 74. Instead of "non-cyst", maybe use "aggregate" or object with no lumen?
We replaced the term "non-cyst" by "aggregate" in the revised manuscript.

* Lines 184-188: unclear
"the culture medium will change color from red-orange to yellow every day after 2 days of incubation…. change medium every 2 days"
So does the medium change color every day or every other day? (even days: red-orange, odd days: yellow)
This line was removed from the manuscript to avoid any ambiguity. Medium changing is done to preserve cell viability throughout the cell culture process.

* Lines 398+: explicit what values are given in the parenthesis, apparently first and third quartile.

The values corresponding to each mathematical magnitude were specified in the revised version (see the Representative results section from line 461.

Reviewer #2:

Manuscript Summary:

In this manuscript, the authors describe a method for 3D characterisation and quantification of biliary cysts.

Major Concerns:

A key aim of this protocol is to enable quantification of cyst generation. While this is performed for cyst number and size, critical endpoints such as cyst viability, function or polarity have not been quantified. These could, in principle, be performed using the same images processed in ImageJ. A potential application of this protocol is comparison of cyst formation in two different hydrogels (eg, Matrigel v a GMP-compatible hydrogel). The ability to quantify viability and function would significant add to the applications of this protocol.

This manuscript aims at showing a protocol to apply a consistent method for quantifying mathematical magnitudes over 3D cell objects in hydrogel. As examples, we provide two mathematical magnitudes with the cyst formation efficiency and cyst size measurements. This manuscript exemplifies the method used in another study, which compares the self-organization potential of NRC cysts in both natural *versus* synthetic hydrogels. In this study, cyst viability and cyst functionality were quantified using the method exposed in our manuscript. Thus, as those quantification results were already published, we invite the reviewer to see the work of (Funfak *et al.*, 2019).

Minor Concerns:

It is not clear from the manuscript how many replicates the data relate to.

How reproducible is the protocol and what are the failure rates?

We thank the reviewer for his/her remarks. Indeed, this information was missing in the previous version of the manuscript but added in the revised version. The reproducibility of the protocol is appreciated thanks to the number of cysts counted on the projections at each time point. In our case, counting a minimum of 200 cysts for the set of projections per day allows to consider that cyst generation has succeeded. To this aim, we added a note from lines 250-253 With this minimum number of cysts counted, we are in a reasonable efficiency error range of ±5% compared to the average. Outside this range, we consider that the protocol failed. However, this estimation about the number of cysts may vary depending on the cell line and the hydrogel type.

How many sets of experiments were performed?

Three independent experiments were performed to characterize biliary cyst formation efficiency and cyst size distribution. This information was provided in the updated version of the legend of figure 4 from lines 543 and 546

Reviewer #3:

Manuscript Summary:

Bouzhir L. and colleague aim at describe a quantitative and reproducible method enabling the generation of 3D epithelial spheroids using biliary epithelial cells as model.

Major Concerns:

Line 252: Section "Quantification of cyst formation efficiency" is difficult to follow and must be better detailed since is the main aim of the manuscript.

In the revised version, we propose a clarified method to explain how we estimate cyst formation efficiency, lines 312-321

The "#cell" in Line 260, refers to the number of cells FDA positive at Day 1 of culture or the number of cells seeded?
The number of cells refers to the number of cells seeded and inferred from the hydrogel volume. This section was clarified from lines 317-319.

What is the rationale behind multiply the "#cysts/cell" for 1000? Are 1000 cells an explicative number or is the number of cells that have been seeded? If so, why they suggest to seed 2.5x105 cells?
We thank the reviewer for noticing this ambiguity. The fact to express the ratio number of cysts/number of cells is just a reference to express the efficiency, which could also be in %.

Line 293/423: How the authors quantify the fluorescence intake and blockage after VP treatment, in correlation with the number of cysts, should be offered.
These quantifications were made in the paper we recently published (Funfak *et al.*, 2019). The same method as the one exposed in the manuscript was used but with an adjustment of the image processing method for fluorescence images. Because of space limitations, we did not detail the procedure in this protocol.

Minor Concerns:
Line 114: spell out "NRCs"
We thank the reviewer for this remark. In the revised version of the manuscript, we defined the acronym earlier in the text when it is first cited on lines 121-122.

*There are no reference of "figure 4A and 4B" in the described section of the manuscript.
The references to the figures 4A and 4B are provided in the section “Formation and characterization of cysts” in the section “REPRESENTATIVE RESULTS” lines 463-468.

*Does the NRCs biliary spheroids maintain the same profile of 2D monolayer culture in term of specific cholangiocytes markers? and in comparison with other 3D hydrogel matrix?
We thank the reviewer for his/her very interesting question. Comparing the setup of the epithelial polarity between 2D and 3D cultures performed in the laboratory, we observed that the cholangiocyte phenotype is further developed in cysts formed in Matrigel compared to 2D cell cultures and other natural and synthetic hydrogels. Early polarity markers such as actin and E-cadherin can be therefore used for the establishment of epithelial polarity in both systems.

We hope you will find this revised version to be suitable for publication in JoVE and would be pleased to provide you with any further information if needed.

Sincerely,

Pascale Dupuis-Williams, Ph.D.
Assistant Professor
pascale.dupuis-williams@universite-paris-saclay.fr
UMR-S 1193 INSERM
Physiopathogénèse et traitement des maladies du foie
Bureau 29 - Bat 443 – Rue des Adèles
Université Paris Saclay, 91405 France

université PARIS-SACLAY

April 15, 2020

Vineeta Bajaj, Ph.D.
Review Editor
Journal of Visualized Experiments (JoVE)
1 Alewife Center, Ste, 200
Cambridge, MA 02140
United States of America

Re: revised-manuscript submission

To: Vineeta Bajaj, Ph.D.

Dear Dr. Bajaj,

We thank you for the revision of our manuscript for publication in JoVE as an original article. Based on the editorial reviews, we are pleased to submit a revised version entitled, “Generation and Quantitative Characterization of Functional and Polarized Biliary Epithelial Cysts”.

We appreciate your suggestions to make our manuscript more concise and didactic. All the modifications have been highlighted in blue in the revised manuscript. Below we are addressing in blue point-by-point your comments.

Answers to the editorial comments

As your article contains detailed, step-by-step, descriptions of software usage, the inclusion of supplemental screen capture or screenshots for the software usage would greatly expedite the scripting and production. You can either take screenshots of the software GUI or use screen capture software (https://www.jove.com/video/5848/screen-capture-instructions-for-authors?status=a7854k). Please include the manuscript number in these supplemental files and number the files in order of appearance: JoVE61404R1_screenfile1, etc.

We have considered your suggestions by including supplementary figures depicting screenshots of the image processing software and modified the manuscript accordingly. Additionally, to greatly expedite the scripting and production of the final movie, movies depicting the quantitative part are also provided. To this aim, we added several references to the supplementary figures from lines 253-298 with their corresponding legends from lines 557-587 The supplementary figures have been uploaded in the naming format suggested by the editor on the JoVE submission site.

1. The editor has formatted the manuscript to match the journal's style. Please retain and use the attached file for revision.

We thank the editor for having formatted the manuscript to match the journal’s style. We considered the attached file for the revision.

2. Please address all the specific comments marked in the manuscript.

Considering the formatted manuscript, we tracked all the editor's edits and addressed all the specific comments. Limitations of our protocol were also added in the discussion section.

3. Once done please proofread the manuscript carefully and ensure that the highlight is no more than 2.75 pages.

We thank the editor for this reminder. While proofreading, we paid attention to ensure that the highlight is no more than 2.75 pages.
We hope you will find this revised version to be suitable for publication in JoVE and would be pleased to provide you with any further information if needed.

Sincerely,

Pascale Dupuis-Williams, Ph.D.
Associate Professor
pascale.dupuis-williams@universite-paris-saclay.fr
UMR-S 1193 INSERM
Physiopathogénèse et traitement des maladies du foie
Bureau 29 - Bat 443 – Rue des Adèles
Université Paris Saclay, 91405 France

Authors Biographies

Pascale Dupuis-Williams is Associate Professor at ESPCI-PSL in Paris and Université Paris Saclay. She received her PhD. in Cell and Molecular Biology for her work in Dr. Beisson's lab at the CNRS, France on tubulin diversity and functions in Paramecium. Dr Dupuis-Williams was a post-doctoral fellow of the European Community.
Dr. Dupuis-Williams' work focuses on liver diseases associated with cilia-related diseases and combines a broad range of molecular, cellular and biochemical approaches. At the head of a the team "Ciliopathies in the liver", she developed 3D biliary organoids models and is responsible for the Work package intended to bio-fabrication of biliary ducts of the Ilite (Innovation in Liver Tissue Bioengineering) project, funded by the French National Research Agency.

Latifa Bouzhir is an engineer in biology (PhD in Molecular Biology, and Protein Bioengineering) in Dr. Pascale Dupuis-Williams team. She works at the French National Institute of Health and Medical Research on a thematic relating to the physiopathogenesis and treatments of ciliopathies and liver diseases. She has integrated a research program related to liver tissue engineering, a very innovative field with the development of bio-engineering of organoids.

Lorena Loarca is a postdoctoral research fellow interested in development of biliary organoids development as an in vitro tool to study organogenesis; disease modeling, and drug studies. Before joining Dr. Dupuis-Williams, Dr. Loarca worked at Mayo Clinic, Rochester, Minnesota, United States at the Laboratory of Dr. Nicholas and at the University of Pennsylvania, Philadelphia, United States, two leading laboratories in the study of biliary diseases.

Emilie Gontran is a postdoctoral research fellow with a scientific background in Biophysics. Since her Ph.D., she worked in physiopathology developing 2D and 3D cell culture models. In her postdoctoral work, she now focuses on biophysical methods, 3D organogenesis models and cell-ECM interactions related to biliary dysgenesis disorders in Dr. Pascale Dupuis-Williams team.

Mauricette Collado-Hilly is an engineer at the French National Institute of Health and Medical Research , who worked on liver physiology with a special focus on calcium signaling with Dr. J.P. Mauger. She then joined the team of Dr. Pascale Dupuis-Williams to take part of the development of biliary models.

2.2.1. Open the Fiji software, open the Z-stack and go to the Fiji menu and click **File | Open**. Select the Z-stack to analyze. If needed, select "**Virtual Stack**" option and click "**Yes**" for opening (**Figure 3A(1)**).

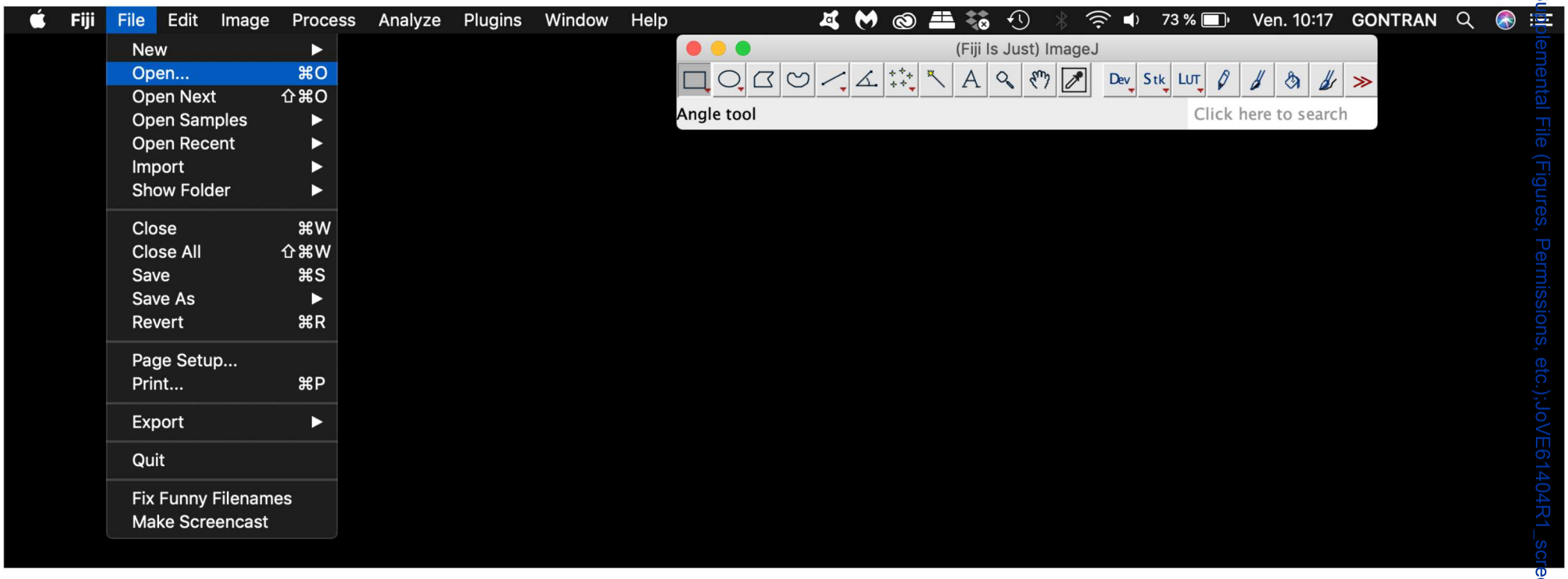

2.2.2. Duplicate the stack via **Image | Duplicate.** Click on the box "**Duplicate stack**" and click "**OK**".

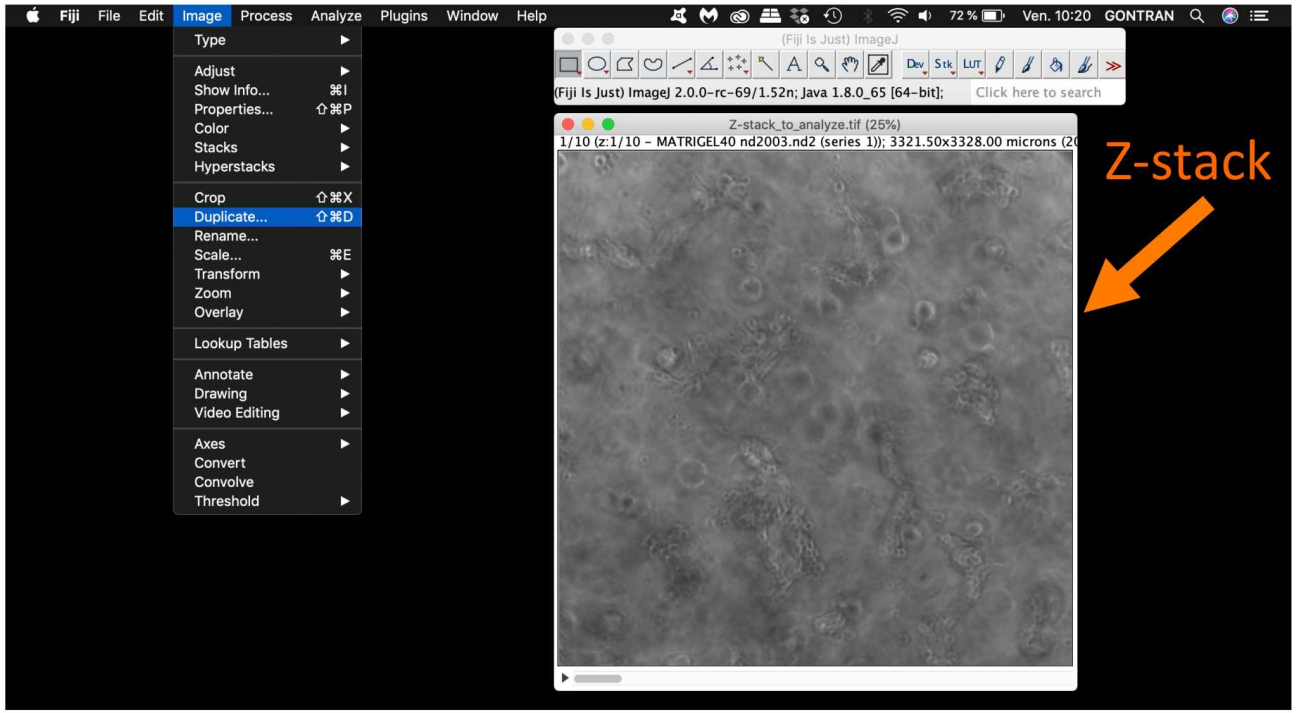

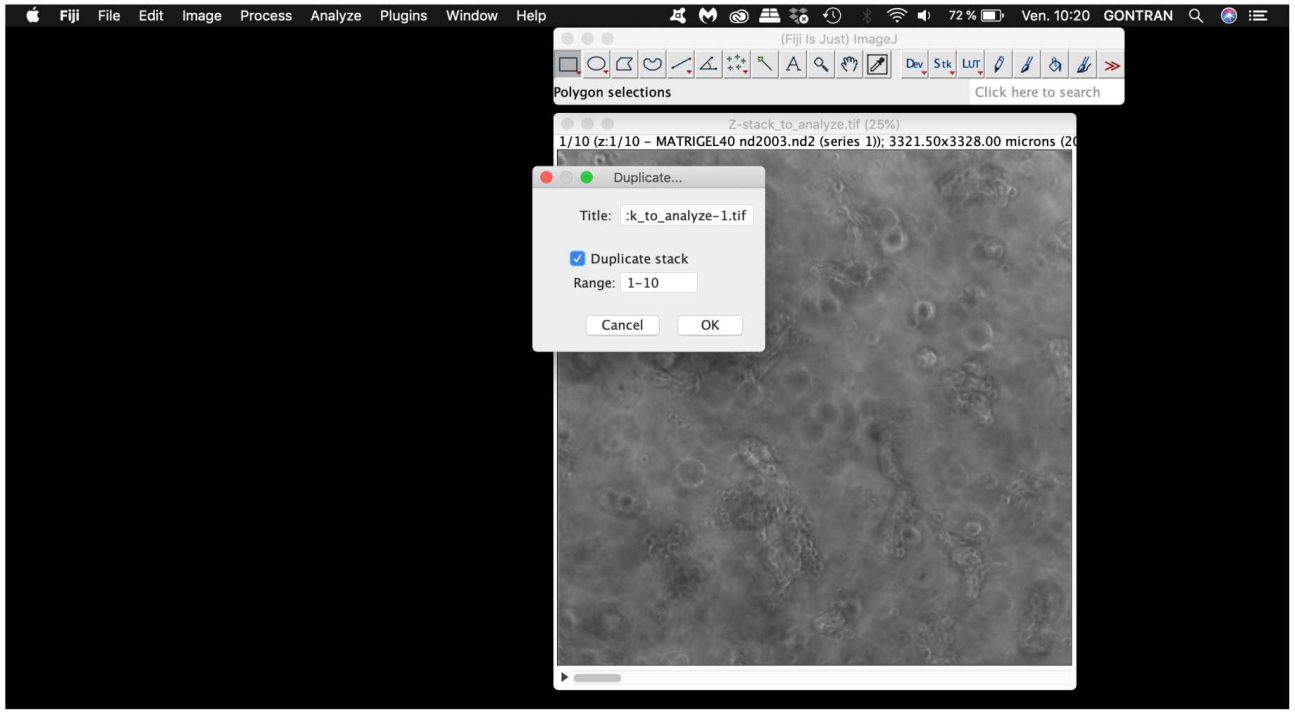

2.2.3. Create a minimum intensity projection from the duplicated stack. Go to the **Image menu | Stacks | Z Project**. Select Projection type "**Min Intensity**" and click "**OK**" (**Figure 3A(2)**).

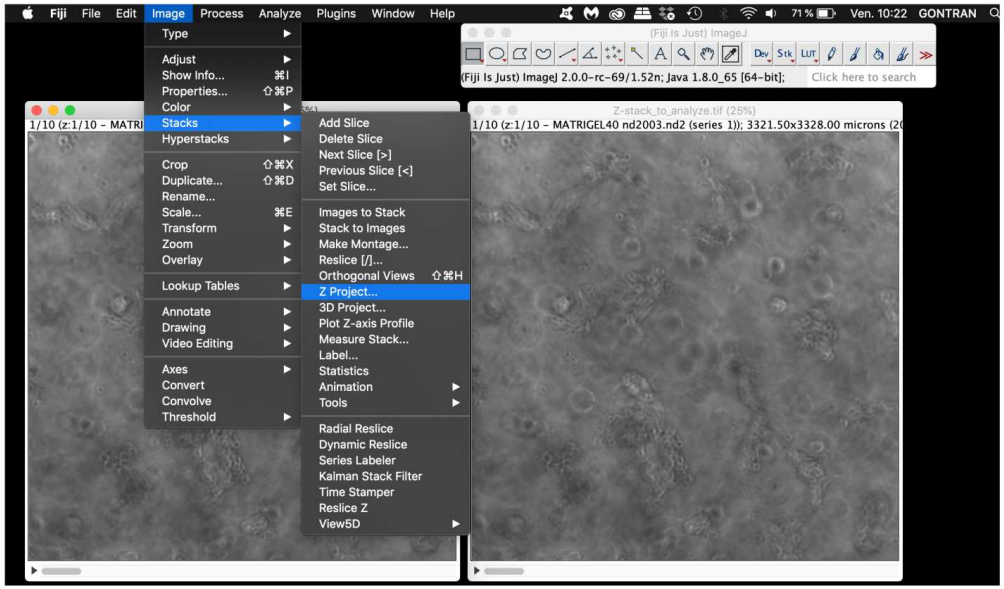

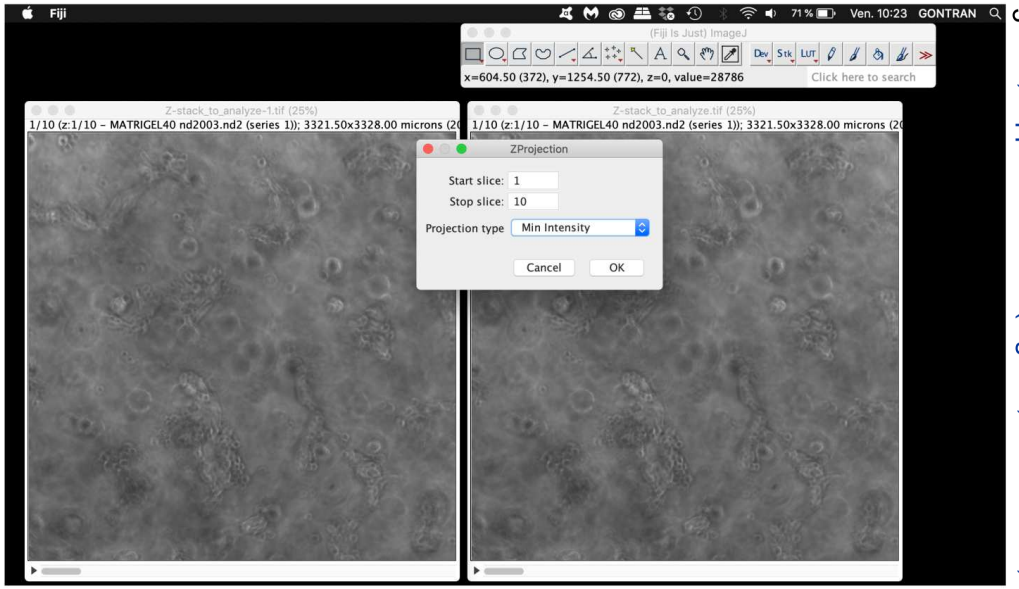

Z-stack projection

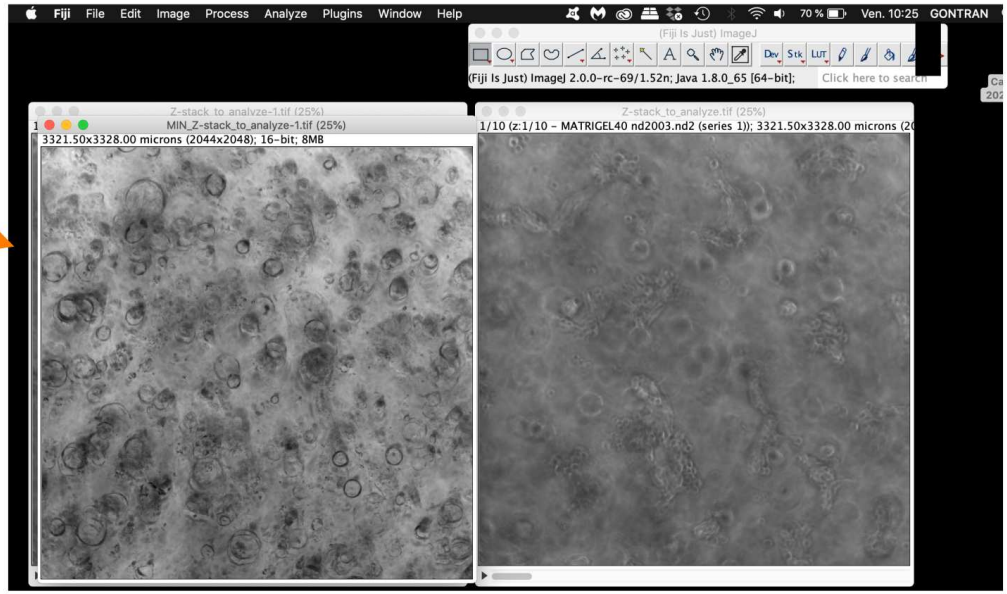

2.2.4. Subtract the background from the projection. Go to the **Process menu | Subtract Background**. Type 500.0 pixels of rolling ball radius and click "**light background**" to render cysts more contrasted than the background (**Figure 3A(3)**).

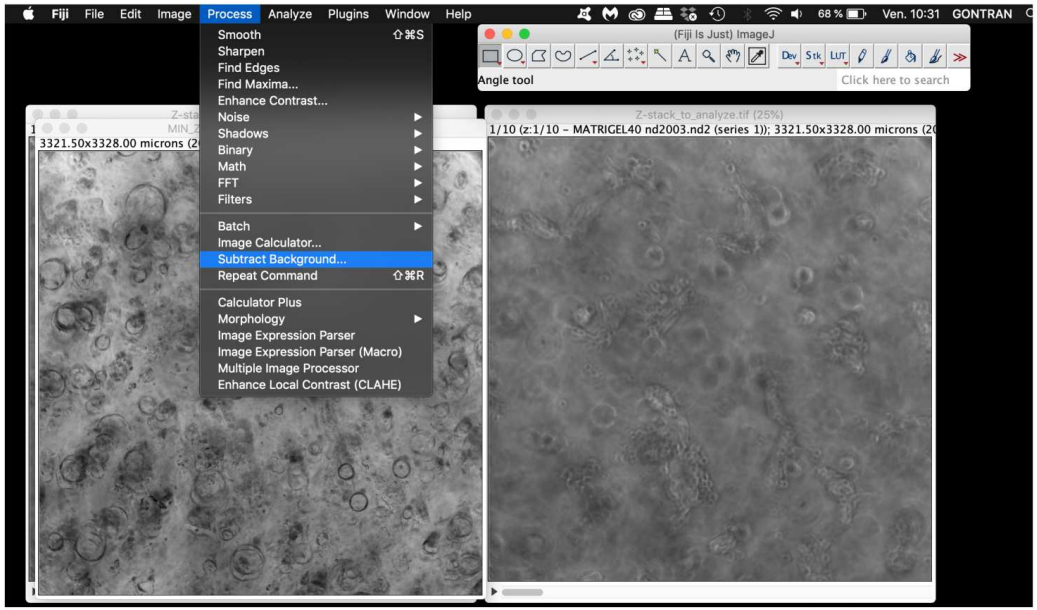

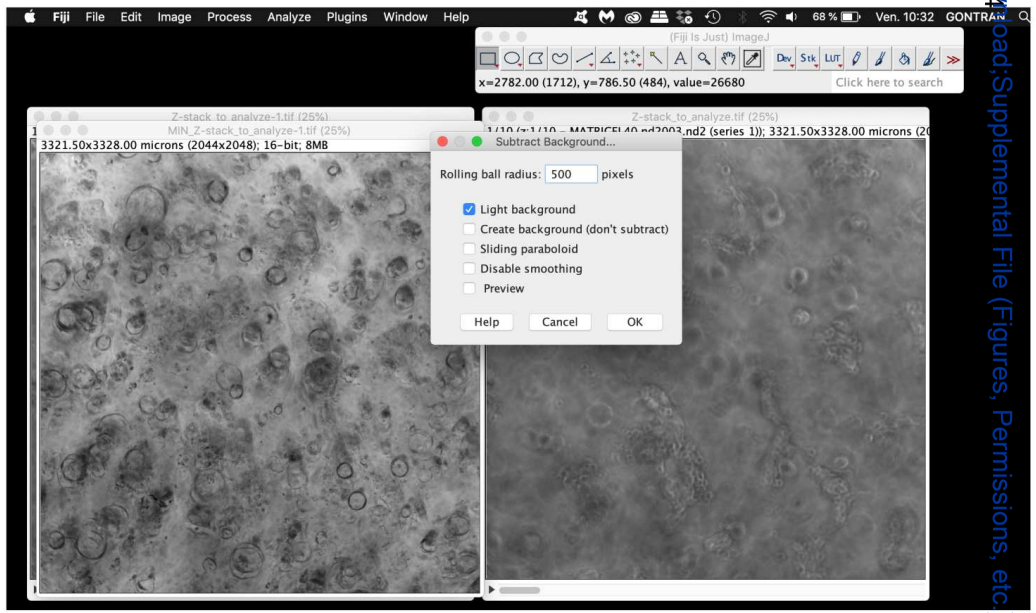

Z-stack projection with subtracted background

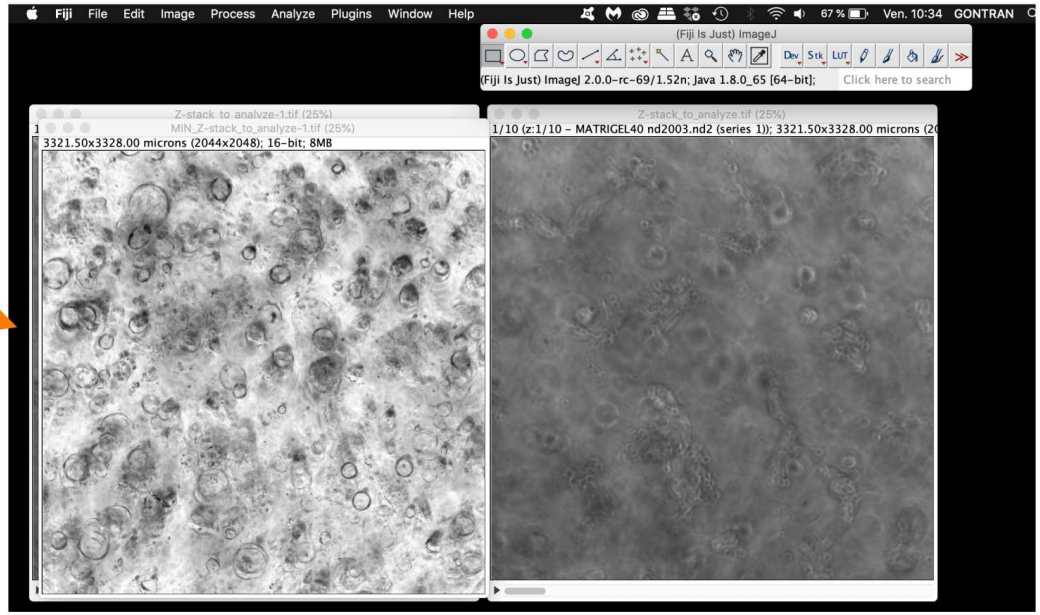

2.2.5. If contrast enhancement is needed, go to **Image menu | Adjust | Brightness/Contrast | Auto | Apply**. Fiji will automatically optimize brightness and contrast. In (**Figure 3A(3)**), the lower and upper gray values were set to 49702 and 65452, respectively.

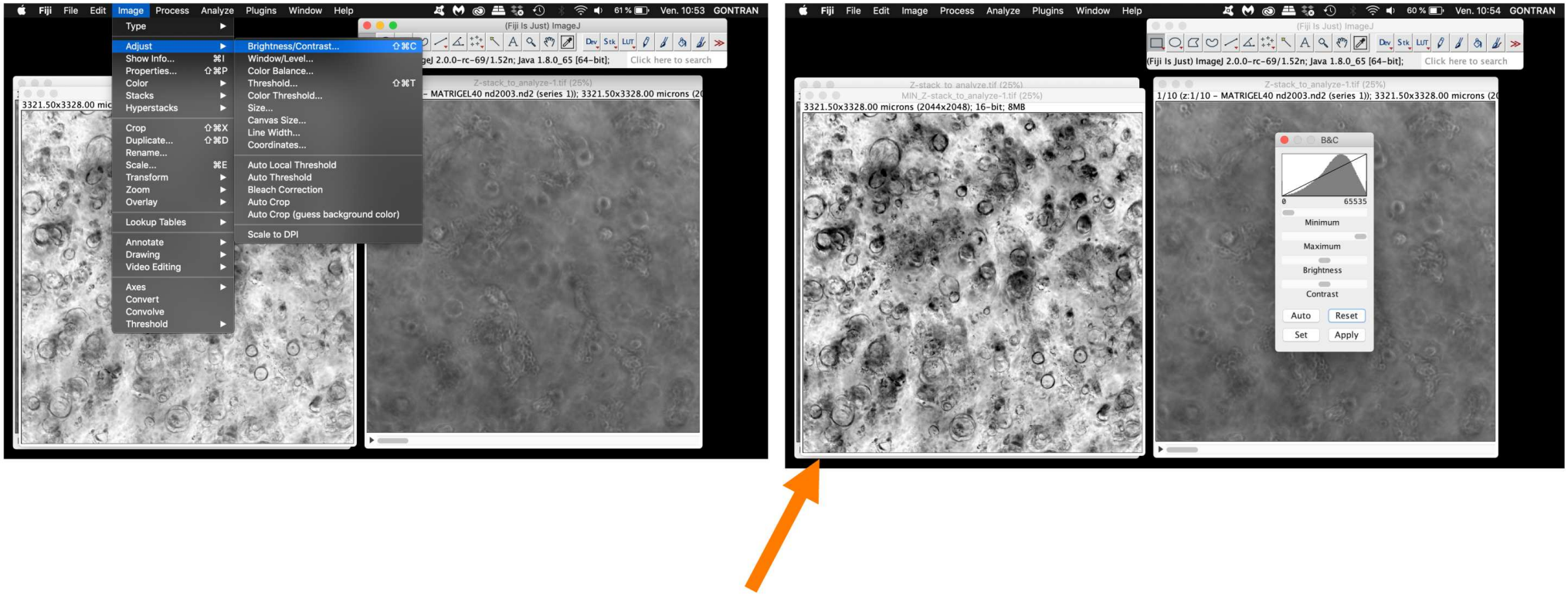

Z-stack projection with subtracted background and contrast enhancement

NOTE: If the projection is not calibrated, go to the **Analyze menu | Set scale** and type the corresponding calibration µm/pixel ratio.

Uncalibrated Z-stack projection

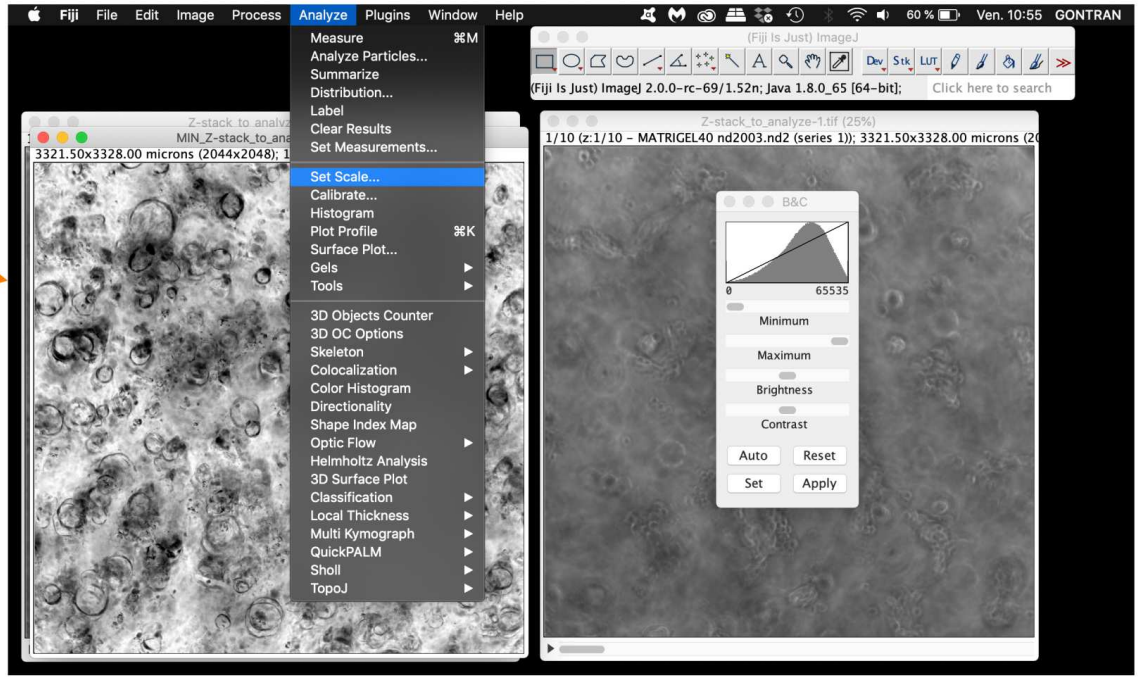

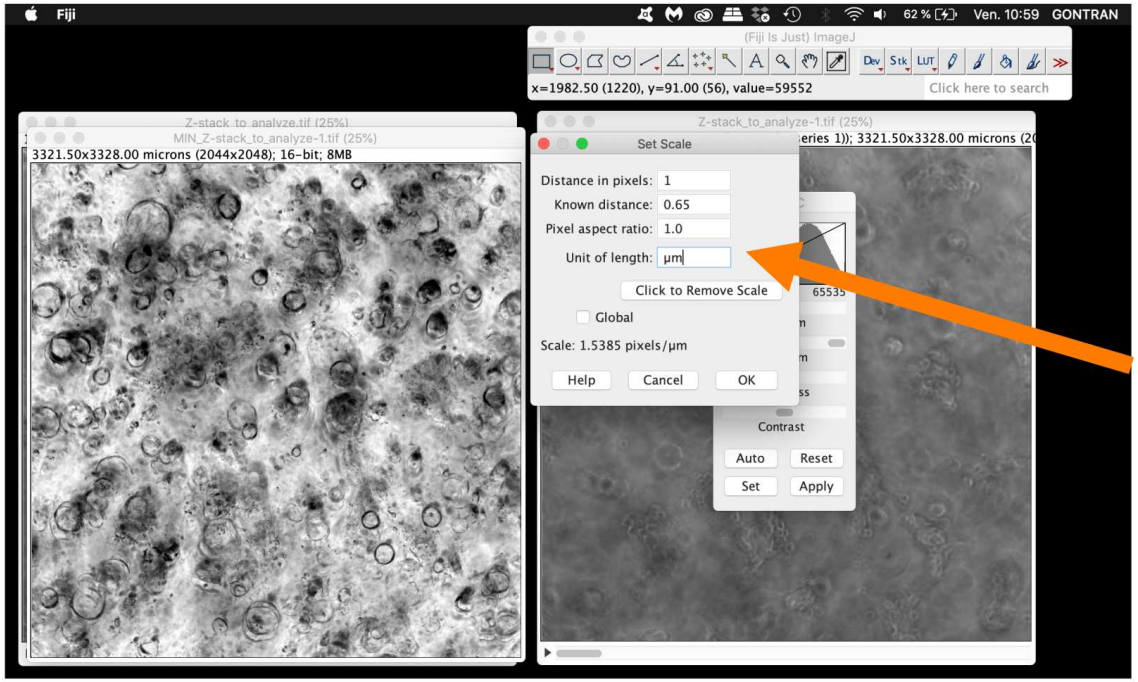

Corresponding µm/pixel ratio used for the calibration

2.3.1. To measure the approximate cyst diameter, select the **Straight-line** tool in the Fiji menu and draw a line across the diameter of each cyst on the final projection (**Figure 3B(4)**). Add the new region of interest (ROI) created for each cyst to the ROI manager: press the "**t**" shortcut on the keyboard for faster counting and opening of the ROI manager.

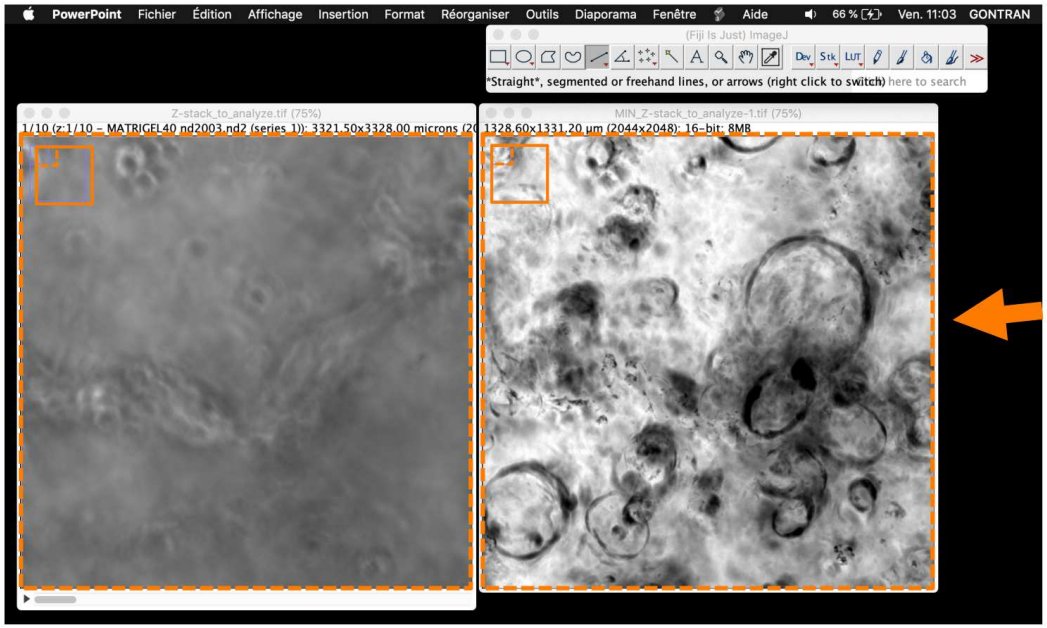

As an example, the analysis of a zoom of the Z-stack projection is given

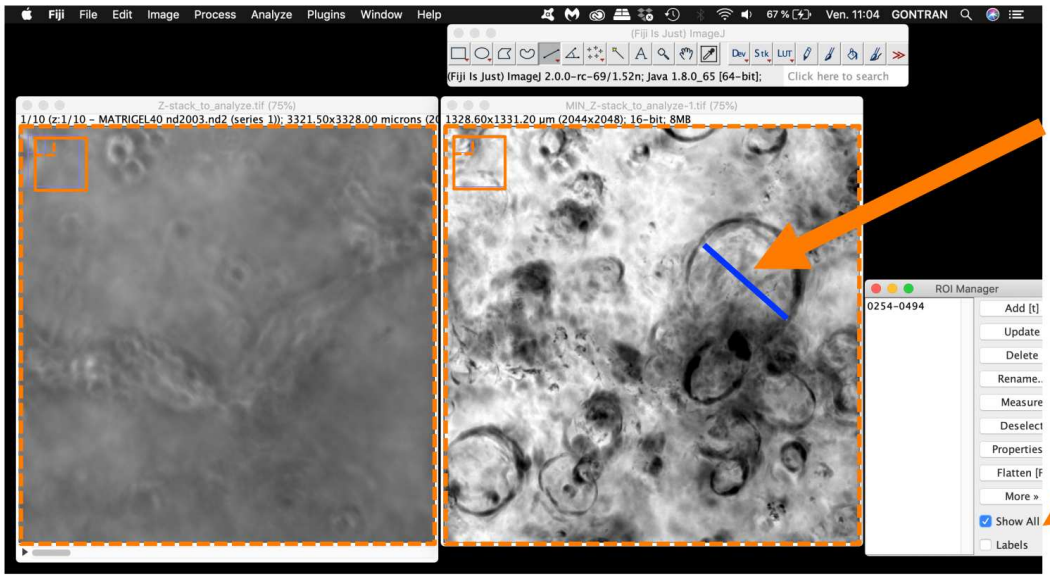

ROI defined (straight-line blue) for cyst counting and cyst size measurement

Click on the "**Show all**" button to see the counted cysts

2.3.2. Check that no cyst has been left without counting by superimposing the set ROIs from the projection on the Z-stack. To do so, click on the **Z-stack window** to select it. In the ROI Manager, click "**Show All**" and move the cursor along the Z-stack to check that image per image, all cysts have been counted.

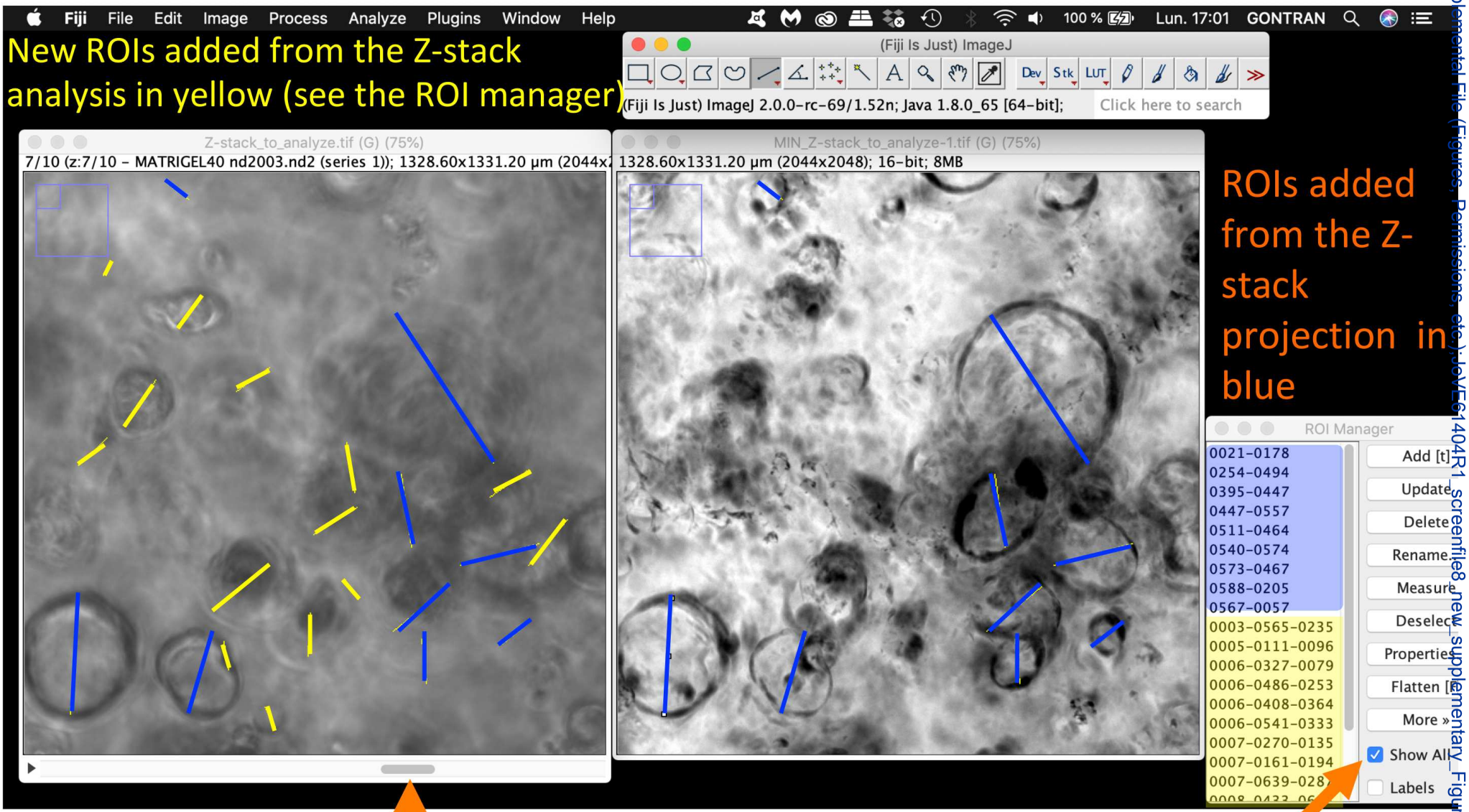

2.3.3. Once new cysts have been counted and ROIs added on step 2.3.1., select the ROI set and save it via the ROI Manager window by clicking **More | Save**.

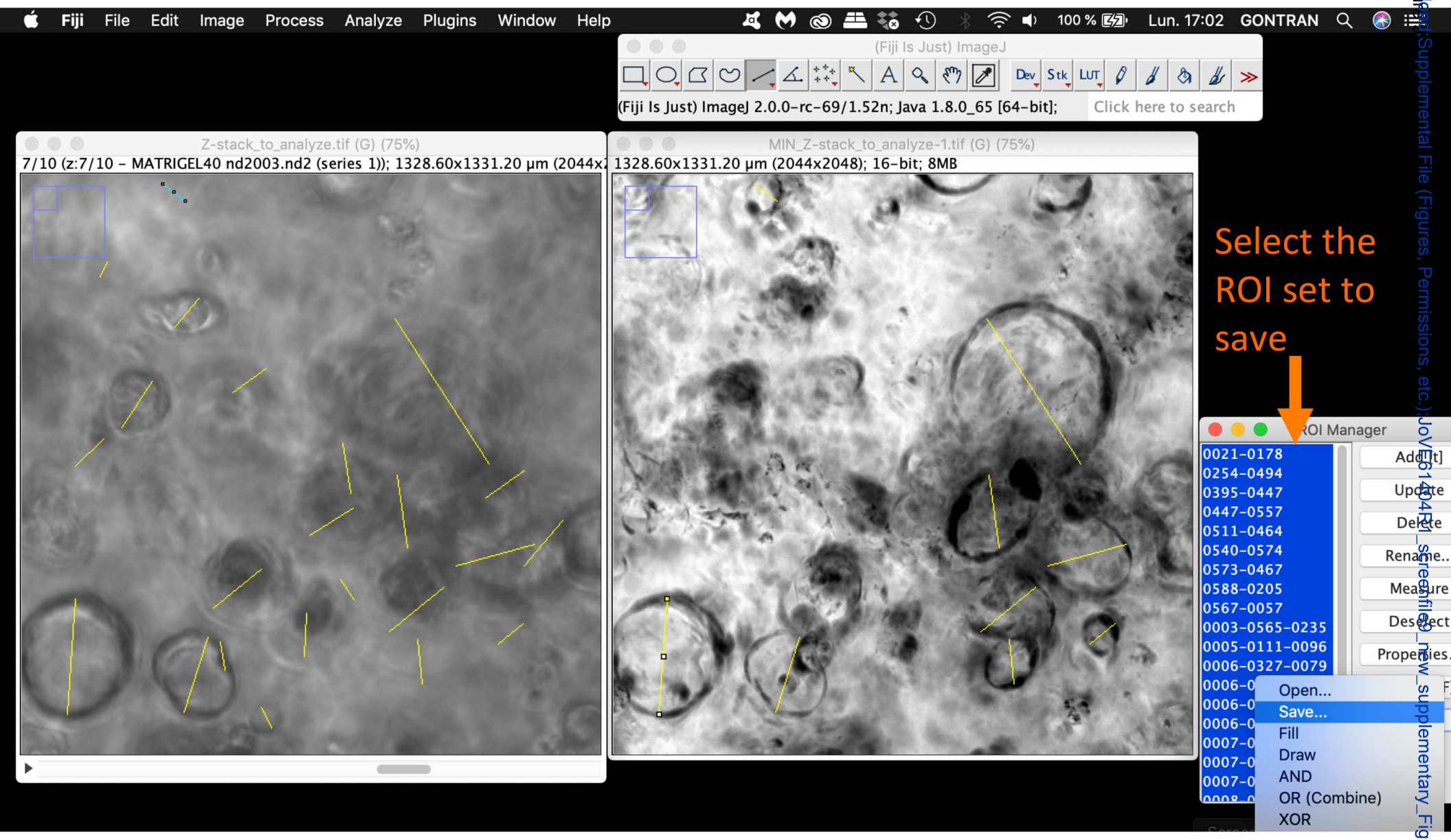

2.3.4. Select all ROIs in the ROI Manager and click "**Measure**" in the ROI Manager to get the size of each cyst. This will open a new window of measurements named "**Results**" numbering each cyst and its estimated size. Then save in .csv format by clicking on the "**Results**" window and via the menu: **File | Save As**.

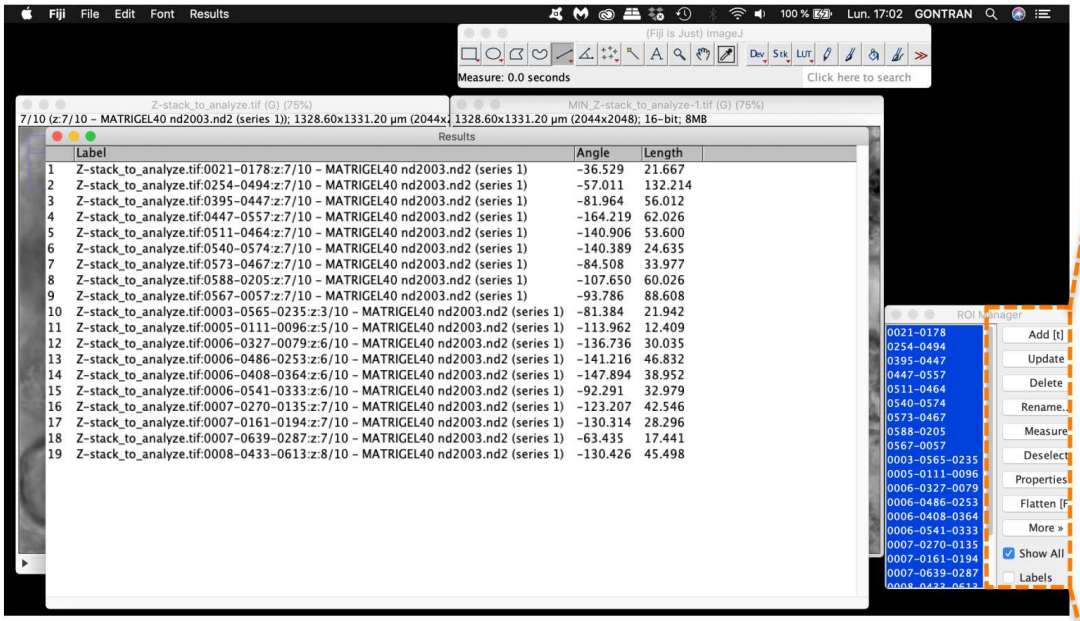

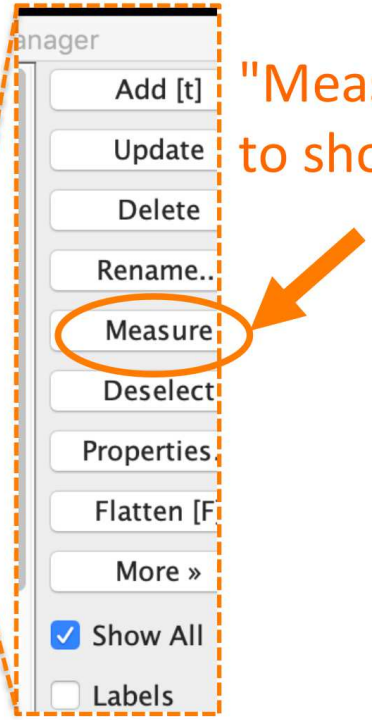

"Measure"button to show the results

Saving of the results